ARMY RESEARCH LABORATORY

Performance Predictions for the ARL Enhanced 2.44-m Blast Simulator

Audrey Mihalcin

ARL-TR-1162 JUNE 1996

Approved for public release; distribution is unlimited.

REPORT DOCUMENTATION PAGE

Form Approved
OMB No. 0704-0188

1. AGENCY USE ONLY *(Leave blank)*	2. REPORT DATE	3. REPORT TYPE AND DATES COVERED
	June 1996	Final

4. TITLE AND SUBTITLE

Performance Predictions for the ARL Enhanced 2.44-m Blast Simulator

5. FUNDING NUMBERS

PR: 68N521

6. AUTHOR(S)

Mihalcin, A.

7. PERFORMING ORGANIZATION NAME(S) AND ADDRESS(ES)

U.S. Army Research Laboratory
Weapons Technology Directorate
Aberdeen Proving Ground, MD 21010-5066

8. PERFORMING ORGANIZATION REPORT NUMBER

9. SPONSORING/MONITORING AGENCY NAME(S) AND ADDRESS(ES)

U.S. Army Research Laboratory
Weapons Technology Directorate
Aberdeen Proving Ground, MD 21010-5066

10. SPONSORING/MONITORING AGENCY REPORT NUMBER

ARL-TR-1162

11. SUPPLEMENTARY NOTES

12a. DISTRIBUTION/AVAILABILITY STATEMENT

Approved for public release; distribution is unlimited.

12b. DISTRIBUTION CODE

13. ABSTRACT *(Maximum 200 words)*

The 2.44-m blast simulator is designed to simulate the blast waveform from an ideal nuclear event. The purposes of this report are to predict the range of equivalent nuclear weapon yields that can be simulated at the facility and to act as an aid for future experimental testing. A quasi-one-dimensional inviscid finite difference hydrocode, known as BRL-Q1D, is used to generate a computational prediction of the blast simulator performance. Based on the facility geometry and maximum rated conditions for the driver tube, peak static shock overpressures are predicted to range from 21.5 kPa to 260 kPa (3 to 37 psig). Static overpressure and dynamic pressure plots, based on BRL-Q1D results, are compared to ideal waveforms to evaluate waveform fidelity. Equivalent nuclear weapon yields are predicted to range from 1.1 kilotons (kt) to 29.0 kt, based on static overpressure impulse, and 0.6 kt to 9.8 kt, based on dynamic pressure impulse.

14. SUBJECT TERMS

blast, nuclear explosion simulation, shock tubes, flow fields, nuclear weapons

15. NUMBER OF PAGES

60

16. PRICE CODE

17. SECURITY CLASSIFICATION OF REPORT	18. SECURITY CLASSIFICATION OF THIS PAGE	19. SECURITY CLASSIFICATION OF ABSTRACT	20. LIMITATION OF ABSTRACT
Unclassified	Unclassified	Unclassified	

INTENTIONALLY LEFT BLANK

ACKNOWLEDGMENTS

The author would like to take this opportunity to thank Mr. Peter Muller, Mr. Stephen Schraml, and Mr. Rich Lottero. Their guidance and patience in answering my many questions was much appreciated. The author would also like to thank Mr. Richard Pearson, Mr. Bernard Guidos, and Mr. John Sullivan for their thorough technical reviews and many constructive comments on improving this report.

INTENTIONALLY LEFT BLANK

CONTENTS

INTENTIONALLY LEFT BLANK

LIST OF FIGURES

PERFORMANCE PREDICTIONS for the ARL ENHANCED 2.44-m BLAST SIMULATOR

1.0 INTRODUCTION

The U.S. Army Research Laboratory's (ARL) 2.44-m blast simulator is a shock tube designed to produce high fidelity simulations of ideal nuclear blast waves. Glasstone and Dolan (1977) use the term "ideal" to describe a blast wave generated over a flat surface that reflects all of the thermal energy and blast that strike it; properties of the blast wave are essentially free of mechanical and thermal effects. Some of the examples that Glasstone and Dolan offer as ideal surfaces include water, ice, packed snow, moist soil with sparse vegetation, and commercial and industrial areas.

This report describes the calculated performance characteristics and yield in kilotons (kt) of the 2.44-m blast simulator. The performance characteristics are then compared to ideal nuclear blast waveforms. The flow field performance of this shock tube is predicted using the BRL-Q1D code (Opalka & Mark, 1986). It is a quasi-one-dimensional computational fluid dynamics code that has proved to be fairly accurate within specific pressure regimes. Using the BRL-Q1D hydrocode, along with analysis of the code run results, this report provides approximate upper and lower pressure and temperature boundaries for future experimental work.

2.0 ARL 2.44-m BLAST SIMULATOR

Glasstone and Dolan cite five main types of burst associated with nuclear blast: (1) air burst, (2) high altitude burst, (3) underwater burst, (4) underground burst, and (5) surface burst. The blast simulator is designed to simulate air burst, defined by Glasstone and Dolan, as a nuclear weapon detonated below 100,000 ft but high enough that the fireball, at its maximum brilliance, does not reach the ground.

The blast simulator was previously referred to as the Ballistic Research Laboratory probative tube. The purpose of the probative tube development program was the development of a research tool for studying new blast simulation techniques. Since the probative tube was similar in many characteristics to the large blast/thermal simulator (LB/TS) constructed by Defense Nuclear Agency (DNA) at White Sands Missile Range, New Mexico (Opalka & Pearson, 1989), the probative tube was also used in the design of the LB/TS and is considered a 1:6 scale model of that facility.

The blast simulator consists of a 2.44-meter diameter expansion tunnel (open to the atmosphere), a 0.91-m diameter driver tube, and a converging nozzle/throat section. Figure 1 is a diagram of the facility. Four major subsystems were added during the probative tube development program completed in 1992 (Pearson, Schraml & Opalka, 1991). These include a cryogenic-based driver gas (nitrogen) supply system, a high pressure driver tube, and a dual diaphragm system. Also attached to the system but not yet fully operational is an active rarefaction wave eliminator (RWE) system to eliminate expansion waves from the end of the shock tube, which would destroy the waveform fidelity in the test section. A thermal radiation source (TRS) is being developed that will eventually be installed to simulate the thermal radiation effects of a nuclear weapon on a target.

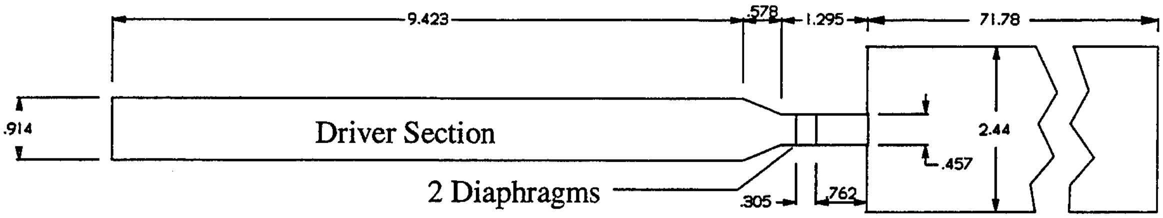

Note: All dimensions in meters - not to scale

Figure 1. 2.44-m Blast Simulator Dimensions.

The test section is located 6.5 diameters from the beginning of the expansion tunnel. Based on equipment ratings, the facility should be able to achieve a driver pressure of 12.8 MPa, gauge (1,850 psig) with a temperature that can reach 700 K (800°F) at maximum driver pressure conditions. Experimental testing is needed and is currently planned to verify these estimates.

This facility creates a shock wave by first filling the driver with high temperature, high pressure nitrogen gas. The end of the driver tube has a converging nozzle section with two diaphragms in the throat. The double diaphragm system is used instead of a single diaphragm fitted with explosive charges since explosives may become sensitized when exposed to high temperatures. The diaphragms are designed to withstand roughly half of the driver pressure and are stocked in different thicknesses for various pressures. The space between the two diaphragms is pressurized to maintain about half the pressure in the driver. The diaphragms are ruptured when the nitrogen gas between the diaphragms is released, causing the differential pressure on the upstream diaphragm to increase until it ruptures. The downstream diaphragm is then exposed to the full driver pressure, causing it to rupture. The driver gas flows into the expansion section, led by a shock wave.

The interface between the driver gas and the shocked air in the expansion tunnel is called the contact surface. To achieve a waveform that simulates the decaying wave of an actual nuclear blast, the density must be similar between the shocked air and expanded driver gas. Glass and Hall (1959) state that pressure and velocity are equal across the contact surface, but density and temperature are usually different. Based on the equation of state for an ideal gas, it is known that a change in temperature directly affects density, which, in turn, affects dynamic pressure. Heating of the driver gas to an appropriate temperature causes the densities of the driven and expanded driver gas to be similar. The heated gas cools as it expands in the expansion section and, if heated properly, will result in density matching across the contact surface. This preheating eliminates an increase in density and dynamic pressure that would result if the driver gas had not been heated.

3.0 METHODOLOGY

The driver tube estimated capability ranges from about 862 kPa, gauge (125 psig) to 12.8 Mpa (1,850 psig) with temperatures reaching 700 K (800°F). These estimates are based on equipment specifications. Based on this range, 11 initial driver conditions were selected for evaluation. The following steps were followed to determine the expected blast simulation performance of the facility:

(a) Initial driver temperature and pressure conditions that produce density matching across the contact surface were determined.

(b) The input file was created. BRL-Q1D was run for the 11 initial driver conditions. BRL-Q1D predictions of static overpressure and dynamic pressure were plotted. Curves for static overpressure and dynamic impulse were created.

(c) Equivalent nuclear weapon yields from Q1D predicted peak static overpressure, static impulse, and dynamic impulse were determined.

(d) Ideal waveforms of equivalent overpressure and impulse were generated to compare to shock tube waveforms and assess simulation fidelity.

The following parts of this section explain each step in greater detail.

3.1 Driver Initial Conditions

The initial driver conditions consist of a desired temperature and pressure within the driver tube. Since pressure was known, it was necessary to calculate an appropriate temperature. This was done using a program called PTUBE (Schraml & Pearson, 1995), which was originally designed for the LB/TS but will also produce accurate predictions for the 2.44-m blast simulator, which is a scale model of the LB/TS.

PTUBE uses the results of computational fluid dynamics analysis and small scale experimentation with a 25.4-cm shock tube to generate empirical relationships between driver gas pressure and temperature. A correct combination of these relationships provides a shock wave of appropriate amplitude to simulate an ideal shock wave with density matching across the contact surface. This program provides an approximation only.

The PTUBE program requires the user to provide the ambient conditions and the desired driver pressure. The program suggests the required driver temperature for approximately matching density across the contact surface and the expected incident shock overpressure at the test section.

3.2 BRL-Q1D Code

The BRL-Q1D code was used to predict static overpressure and dynamic pressure histories produced by the 2.44-m blast simulator. This code uses quasi-one-dimensional, adiabatic, inviscid, numerical algorithms to solve the Euler equations (Opalka & Mark, 1986). The option to use a Beam and Warming implicit finite difference technique in the code was used instead of the option to use the MacCormack explicit finite difference technique. The implicit numerical scheme is less sensitive to area changes and is more stable than the explicit scheme in this code according to Opalka and Mark. During the original development of this code, experimental data were used to validate its ability to model transient flow in shock tubes. The grid for these runs has a total of 1600 points. Figure 2 illustrates the configuration of the BRL-Q1D model and the grid distribution within the model. The code clusters grid points in critical areas by superimposing a fine grid over a basic course grid. Only a small part of the expansion section is shown, but the grid spacing remains constant from where the grid grows larger in the expansion section to the shock tube exit.

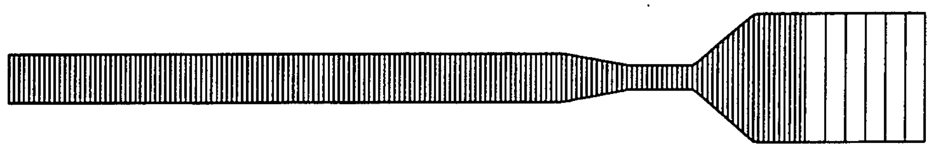

Note: Does not include full exapnsion section

Figure 2. Grid Distribution.

BRL-Q1D has proved to be a reliable code but with some limitations. A one-dimensional code can only give approximate results of the flow simulation since the actual flow is three dimensional. The Q1D code is referred to as a quasi-one-dimensional code because it allows limited area changes. Abrupt area changes cause the code to become unstable. The exit of the throat section of the 2.44-m blast simulator has a sudden area change as can be seen in Figure 1. In the BRL-Q1D model, the driver, converging nozzle and throat section are modeled to identically match the actual facility. Setting up the grid configuration to avoid abrupt area changes required allowing for an angled, diverging nozzle section to create a more gradual area change. This 45° diverging nozzle, as can be seen in Figure 2, was added to the end of the throat section, extending to the 2.44-m diameter expansion tunnel.

The actual facility has a double diaphragm system. For the purpose of running the code, though, a single boundary was set up at the location of the upstream diaphragm separating the heated, high pressure gas from ambient conditions. This approximation is acceptable since any perturbations in the flow caused by a double diaphragm system will have little effect on the primary flow at the test section.

A rarefaction wave is an expansion wave that is caused by the shock front encountering an abrupt area change going from the expansion section to the surrounding atmosphere. The rarefaction wave travels upstream, in the opposite direction of the flow, in an attempt to bring the under-expanded driver gas back to ambient pressure. When the rarefaction wave reaches the test section, the static pressure decreases and dynamic pressure increases as fluid particle velocity increases. An RWE reduces the area of the exit, which accelerates the flow and reduces the static pressure of the blast to ambient. Because there is no pressure difference, no expansion wave is created. This effect, of a properly working RWE, simulates an infinitely long expansion section. The BRL-Q1D model of the expansion section was made sufficiently long to eliminate the effect of a rarefaction wave.

3.3 Yield Calculations

Nuclear weapon yield calculations were performed using a program described by Schraml and Pearson (1995) called YIELD. The program is based on the Reflect-4 Code (Smiley, Ruetenik, and Tomayko, 1982). This code uses Sachs' scaling to fit a tabulated reference blast wave based on a 40-kt blast to user data. The program takes user-supplied inputs for peak static overpressure, static overpressure impulse, ambient pressure, ambient temperature, and dynamic pressure impulse and provides equivalent ideal nuclear weapon yields. Care must be taken in selecting peak static overpressure. At mid-level and lower pressures, minor changes in peak static overpressure can cause significant differences in calculated yield. Selecting a lower peak static overpressure but maintaining the same static overpressure impulse and dynamic pressure impulse will cause the yield to be higher since, in effect, it would require a larger nuclear weapon to create the same effect at a greater distance.

3.4 Ideal Waveforms

The ideal waveforms generated by a program called BLAST (Schraml and Pearson, 1995) are used to compare predicted blast wave histories to ideal nuclear blast waveforms. The program uses a modified Friedlander equation of the form

$$p(t)=p_{max}*(1-t/ppd)*e^{-ci*t/ppd}$$

in which

p = static overpressure

t = time

p_{max} = amplitude of incident shock

ppd = positive phase duration of the blast

ci = decay constant of the blast wave

The user prescribes the peak static overpressure, yield, ambient pressure and ambient temperature. The program calculates the equivalent height of burst of the weapon, equivalent ground range to the observation point, and static overpressure and dynamic pressure as a function of time.

4.0 DATA ANALYSIS

Table 1 is a summary of the results of the 11 Q1D code runs. As stated before, these runs were set up to simulate the expected operating range of the 2.44-m blast simulator. Shock overpressures and yields are at the test section.

Calculations are based on an ambient pressure of 101.35 kPa (14.7 psi) and an ambient temperature of 288.71 K (60° F). "Shock Overpress. (kPa)" is the peak static overpressure.

"Yield - Static (kt)" and "Yield - Dynamic (kt)" refer to equivalent nuclear weapon yields, based on static overpressure impulse and dynamic pressure impulse, respectively.

Table 1

Summary of Results

Driver Pressure (kPa,gauge)	Driver Temp. (K)	Shock Overpress. (kPa)	Yield - Static (kt)	Yield - Dynamic (kt)
862	312.6	21.5	1.11	0.61
1207	324.8	28.8	1.64	0.86
1551	337.6	36.5	2.17	1.06
2068	356.5	46.5	2.95	1.47
2758	378.7	60.5	4.28	1.87
3792	406.5	78.5	6.92	2.69
5171	442.6	107.0	10.29	3.16
6205	459.8	128.0	12.32	3.29
8274	494.8	175.0	16.54	4.81
10342	529.3	215.0	20.16	6.88
12755	567.0	260.0	28.98	9.79

4.1 Procedure/Assumptions

For each of the 11 Q1D code cases, the following data were plotted:

(a) Static overpressure (kPa).

(b) Static overpressure impulse (kPa-s).

(c) Dynamic pressure (kPa).

(d) Dynamic pressure impulse (kPa-s).

(e) Ideal waveform derived from static overpressure impulse.

(f) Ideal waveform derived from dynamic pressure impulse.

Analysis of these results required making some assumptions in order to interpret them consistently. As mentioned earlier, choosing peak static overpressure is important in order to achieve consistent results in determining yield as well as shock strength. These assumptions are

a. The peak static overpressure impulse is determined to be the impulse at the conclusion of the first positive phase. Some of the cases at higher pressures do not exhibit a negative phase within the time frame of interest. In these cases, the peak static overpressure impulse is determined to be the cumulative impulse as of 700 ms. The actual code runs are extended to 1 second. By terminating the impulse calculation at 700 ms, less than 2% error is introduced in the yield calculations. This is judged to be acceptable for this series of runs, since, as time passes, the static overpressure is so low as to be considered insignificant in its ability to be destructive.

b. Since it is known that the BRL-Q1D code overshoots the initial static overpressure peak, this value was determined by inspection. The vertical distance between the two highest peaks was measured and the peak was estimated to be approximately one third of that distance higher than the lower of the two peaks.

c. The peak dynamic pressure, q, is the kinetic energy per unit volume of air immediately behind the shock front. For this report, q is defined as

$$q=\frac{1}{2}\rho u^2$$

in which ρ=density, kg/m^3

u=particle velocity, m/s

4.2 Analysis

Weapon yields based on static overpressure impulse and dynamic pressure impulse do not match the equivalent free field yields in a shock tube (Opalka, 1987). This is because a free field, spherical explosion has different static and dynamic impulse relationships than does a simulated blast produced in a linear direction inside a shock tube. Therefore, calculations also include yield based on dynamic pressure impulse. Both static overpressure and dynamic pressure are important. Effects of static overpressure can cause damage because of crushing in the diffraction phase of the event, while dynamic pressure effects can include damage by overturning caused by drag loading.

Figure 3 shows the predicted operating curve for yield versus shock overpressure at the test section. Based on calculated results, the blast simulator is capable of having yields as high as 28 kt with expected peak shock overpressures of 260 kPa (37 psig). BRL-Q1D predictions of flow in other shock tubes with similar configurations have greatly over-predicted high pressure shots (Opalka, 1987). Shock overpressures above 140 kPa (20 psig) will require much higher driver overpressures than those predicted by Q1D (Opalka, 1987). It is expected that 172 kPa (25 psig) will be the actual maximum static overpressure of the facility's capability. The computations also predict that this facility can produce yields based on dynamic pressure as great as 9.79 kt. Experimental testing is expected to illustrate a gradual divergence of experimental and predicted results. In the past, the expected divergence of experimental and predicted results has proved to be attributable to the BRL-Q1D code over-predictions and experimental variations, which can cause significant differences at higher pressures. The actual point at which the code can no longer adequately predict actual shock tube performance can be determined once experimental data are available.

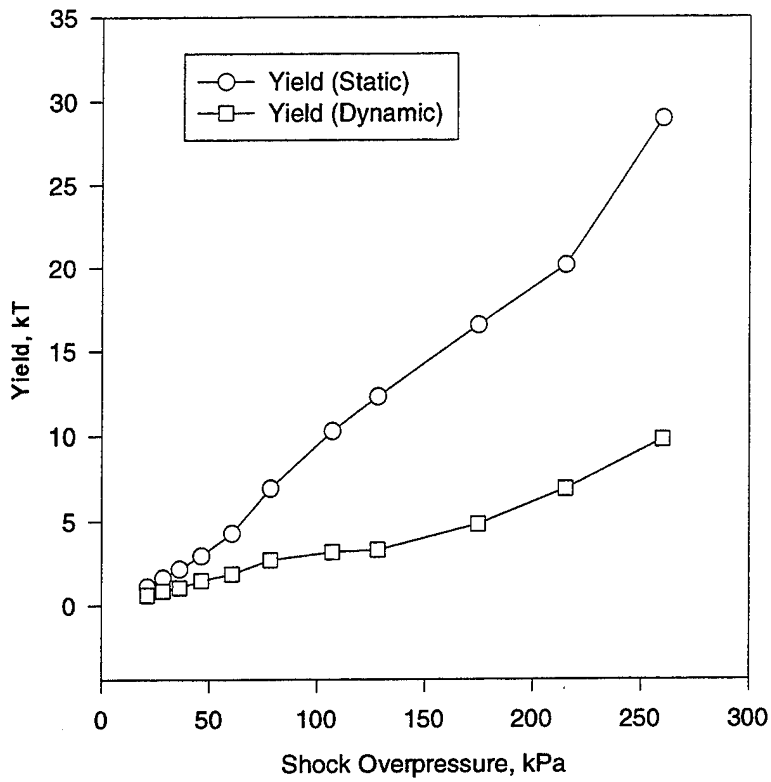

Figure 3. Yield Versus Shock Strength.

Figure 4 shows the predicted operating range of the driver and its relationship to yield. To attain the 28.98-kt range, the driver tube must reach overpressures as great as 12.75 MPa (1850 psig) at a temperature of 567 K (560° F). This is on the upper end of the gas-handling system's capability.

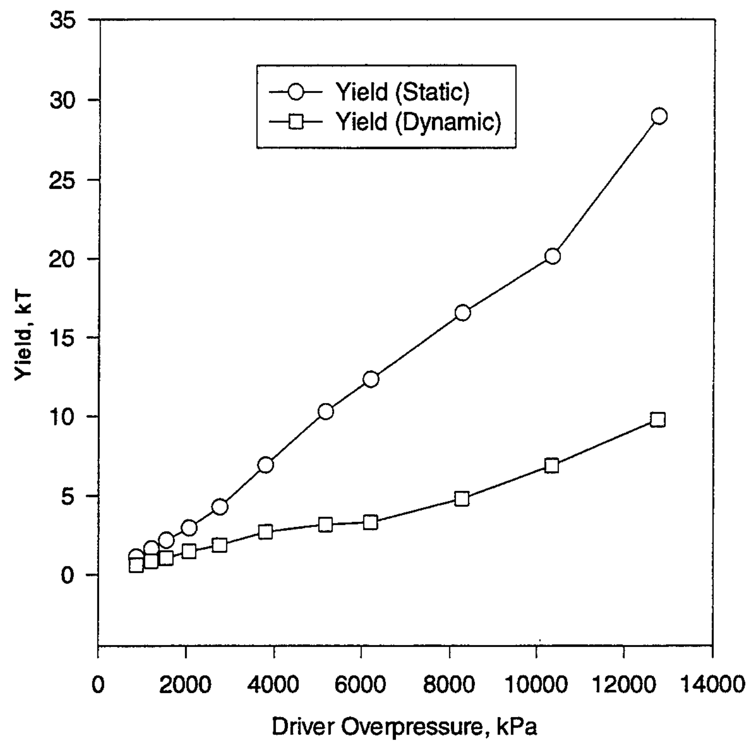

Figure 4. Yield Versus Driver Overpressure.

Figures 5 through 26 are plots of the code run results. These figures start on page 19. Each driver condition is represented by two figures. The first figure in each pair compares ideal waveforms to predicted static overpressure and dynamic pressure. These ideal waveforms are based on weapon yield developed using static overpressure impulse. The second figure in each pair compares ideal waveforms, based on weapon yield developed using dynamic pressure impulse to calculated static overpressure and dynamic pressure plots.

For Figure 5, which corresponds to a driver overpressure of 862 kPa (125 psig), shows that the static overpressure positive phase duration ends 0.48 second into the event. Flow through the throat section of the shock tube is sonic and therefore limits the mass flow rate through the nozzle. Since this driver condition has the lowest pressure and therefore the lowest mass flow rate, the positive phase duration is the shortest of all the driver conditions. The ideal waveform corresponds well with the predicted waveform for static overpressure. This is to be expected since the development of an ideal blast waveform is based on the static overpressure and dynamic pressure waveforms based on BRL-Q1D static overpressure impulse. Thus, the ideal blast wave must have the same impulse as the static overpressure waveform.

The lower plot of Figure 5 compares dynamic pressure to an ideal waveform for dynamic pressure. The ideal waveform is based on yield calculated from static overpressure. As mentioned earlier, a blast from a shock tube does not simulate the same relationship between static overpressure and dynamic pressure as in an actual free field nuclear event. Dynamic pressure from a real nuclear event has a longer positive phase than static overpressure (Glasstone & Dolan, 1977). In general, this effect is only a few percent at lower overpressures but can be more than twice as long at extremely high overpressures. The plot shows that the ideal waveform does not correspond with the dynamic pressure record. The area under the curve for dynamic pressure is obviously less than for the ideal waveform.

Figure 6 plots are at the same driver condition as in Figure 5 and they have the same static overpressure and dynamic pressure histories generated by BRL-Q1D. The ideal waveforms on this page are developed from weapon yield based on dynamic pressure impulse, peak static overpressure, ambient pressure, and ambient temperature. The static overpressure is higher than the ideal waveform and is not a good fit. However, the plot comparing dynamic pressure to the ideal waveform is a good fit since the waveform is based on dynamic impulse. If there were a significant problem with density matching of the contact surface, the dynamic pressure records would not correspond well with ideal waveforms.

All the figures will have the same results when static and dynamic plots are compared with ideal waveforms. That is, static overpressure plots will correspond well with ideal waveforms that are based on weapon yield calculated from static overpressure impulse; however, the dynamic counterpart will not match the ideal waveform since the blast wave from the shock tube cannot simulate a true nuclear event in both static overpressure and dynamic pressure in only one shot. The same situation exists when the plots are compared to ideal waveforms, based on weapon yield from dynamic pressure impulse, except the reverse will be true. The dynamic pressure plots will match with the ideal waveforms, while the static overpressure plots will not correspond well.

All the figures show the stair-step pattern characteristic of blast from a single driver shock tube. These steps are the effects of reflections of the expansion wave from the upstream end of the driver tube and the effect of having a converging section. A target would not be significantly influenced by this stair-step effect.

From Figure 15 until Figure 26, the highest test condition, the positive pressure phase for static overpressure has extended past the time period of interest. This is because of the large amount of mass emptying from the driver tube at driver conditions of 3.79 MPa (550 psig) and above. The plots were not extended in time because as the static overpressure approaches zero kPa, there is little potential in the remaining history to inflict damage to a target. In a real nuclear event, the dynamic positive phase would be longer than the static overpressure positive phase and the time period of interest would be longer.

Figures 19 to 26, 175 kPa to 260 kPa (25 to 37 psig) shock overpressures, show an interesting effect that is not found in a nuclear event. Opalka (1987) has shown that with a similar shock tube configuration, recompression shocks are generated within the Q1D code for shock overpressures of 170 kPa and above. A recompression shock forms in the nozzle and breaks free when there is a large enough pressure ratio, usually above 40 (Opalka, 1991). For an interval of 0.23 s to 0.34 s, depending on the driver conditions and shock strength, a recompression shock occurs and its effects can be seen at the test section. For Figures 19 and 20, the effects of the recompression shock can be seen about 0.23 s into the event. The recompression shock is indicated by a sudden spike in static overpressure with a small spike in dynamic pressure. Some previous research (Opalka, 1987) indicates that although the recompression shock exists, Q1D over-predicts the strength of it as well as the location. For this particular facility, the recompression shock occurs at the end of the period of interest and has minimal effect on the target but may have a minor effect on the calculation of yield since impulse is affected. It is anticipated that experimental testing will show that the very high shock strengths will not be attainable; therefore, recompression shocks would not be an issue.

5.0 CONCLUSIONS

These results provide an indication of the wide range of shock overpressures and equivalent weapon yields that the 2.44-meter blast simulator is capable of producing. There are two important points to be stressed about these results. One is that the predictions are based on a one-dimensional code. Although this code can approximate the flow, it is not as reliable in predicting shock tube phenomenology as a three-dimensional code. The other point is the need for experimental work to confirm predictions or provide more accurate results, especially at higher driver pressures. The operating curves presented are only an estimate until the facility is characterized.

A summary of the results of this report is as follows:

1. The enhanced 2.44-m blast simulator does not produce the same relationship between static and dynamic waveforms as is found in the blast waves from actual nuclear detonations. This inability to reproduce the proper relationship means that the simulated weapon yields calculated, based on static and dynamic impulse, differ in the blast simulator. If there were an interest in seeing the effects of diffraction loading and drag loading on a target for one specific weapon, two tests at different driver pressures would be necessary.

2. Predicted shock strengths range from 21.5 kPa (3.12 psig) to 260 kPa (37.71 psig), though the high end of the range is optimistic.

3. Yield based on static overpressure and impulse ranges from 1.11 kt to 28.98 kt. Yield based on static overpressure and dynamic impulse ranges from 0.61 kt to 9.79 kt. Since predicted shock strengths for higher driver pressures and temperatures are optimistic, actual yields may differ significantly.

4. The predicted recompression shock that occurs at the high temperatures and pressures is over-predicted by a 1-D code and either does not exist or is much weaker than the code indicates. It should have minimal or no effect on dynamic and static pressures.

5. Accurately interpreting peak static overpressure from Q1D code runs is critical for properly determining kiloton yields, especially at low to mid shock strengths.

At a minimum, the rarefaction wave eliminator must be operational in order to achieve a high fidelity nuclear blast simulation. Without it, the rarefaction wave from the end of the expansion section will destroy the simulation before the time period of interest has ended. Also, the thermal radiation source (TRS) is important to simulate a nuclear event. Without it, the face of the target may not be properly impacted since the TRS' high temperature degrades the surface of a target.

The data and predictions presented here are based on a one-dimensional code. Ensuing work with a two- or three- dimensional code would improve the accuracy of computational results and should provide a more realistic numerical flow simulation. Numerical flow simulations are important since not all flow characteristics can be experimentally measured.

Experimental work is also necessary to find the true upper and lower mechanical limits of the driver fill system. Specifically, the maximum combined temperature and pressure conditions are not known. Also, the double diaphragm system has not been proved at high pressures and temperatures and may be a limiting factor.

This work should only be considered an attempt to predict the capabilities of this facility. It can also be used as an aid in setting up a test plan for experimental characterization. During and after experimental testing, a comparison should be made to validate the testing and to provide verification of the applicability of BRL-Q1D code to this facility.

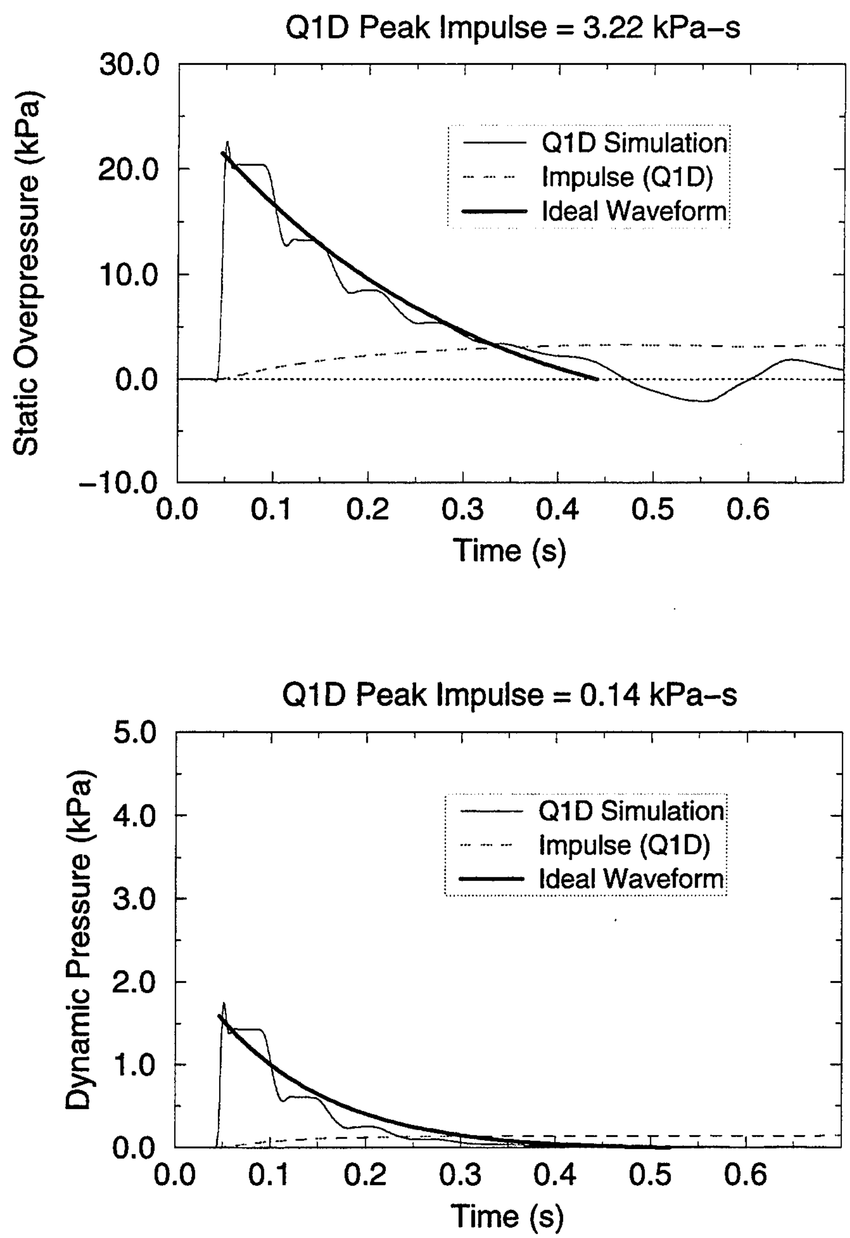

Figure 5. 862 kpa (125 psig) Driver Overpressure - Ideal Waveform Based on Static Overpressure Impulse.

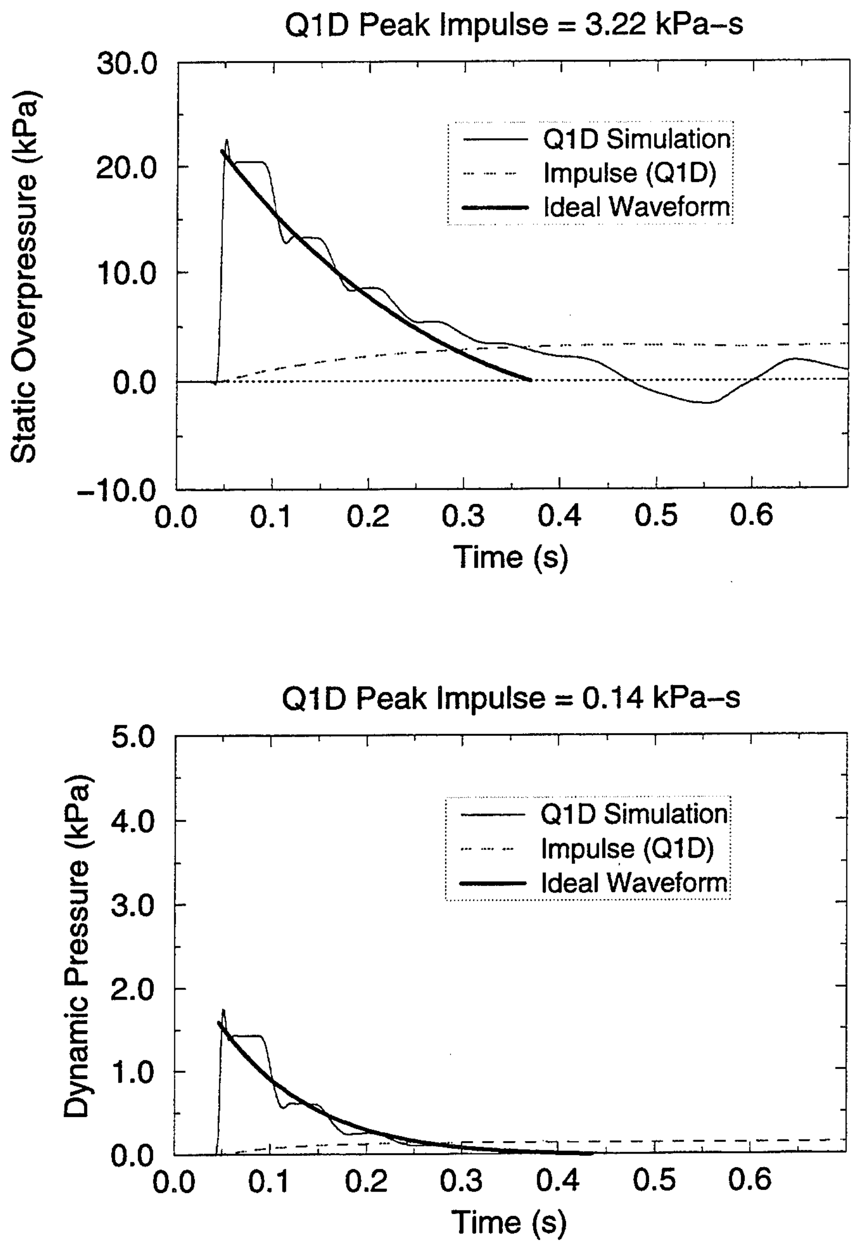

Figure 6. 862 kPa (125 psig) Driver Overpressure - Ideal Waveform Based on Dynamic Overpressure Impulse.

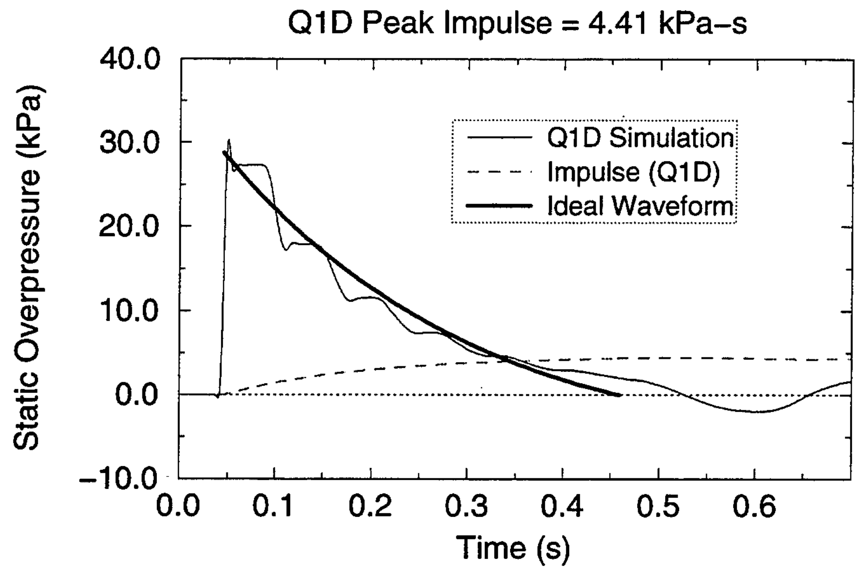

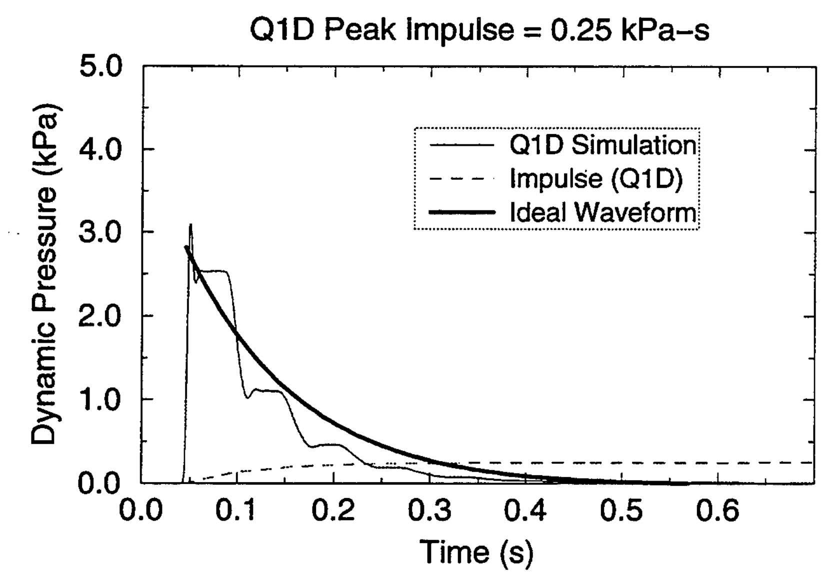

Figure 7. 1.21 MPa (175 psig) Driver Overpressure - Ideal Waveform Based on Static Overpressure Impulse.

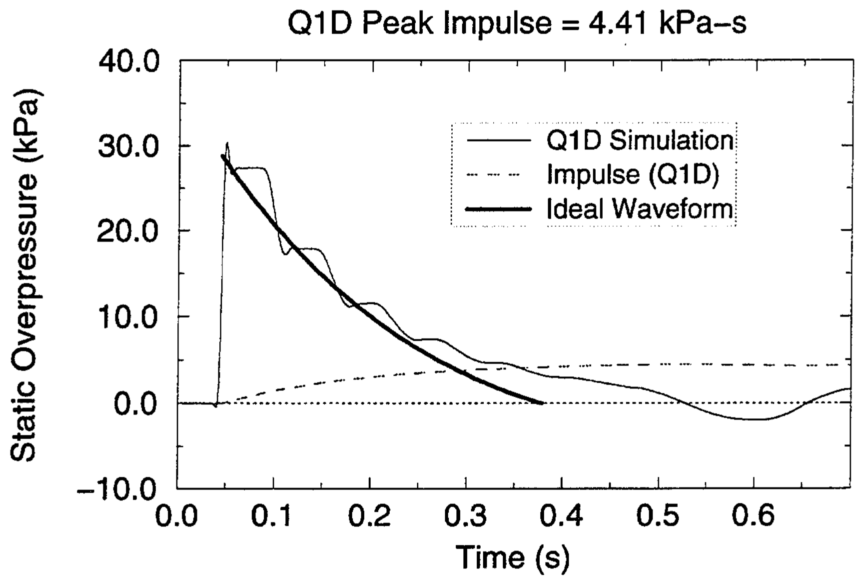

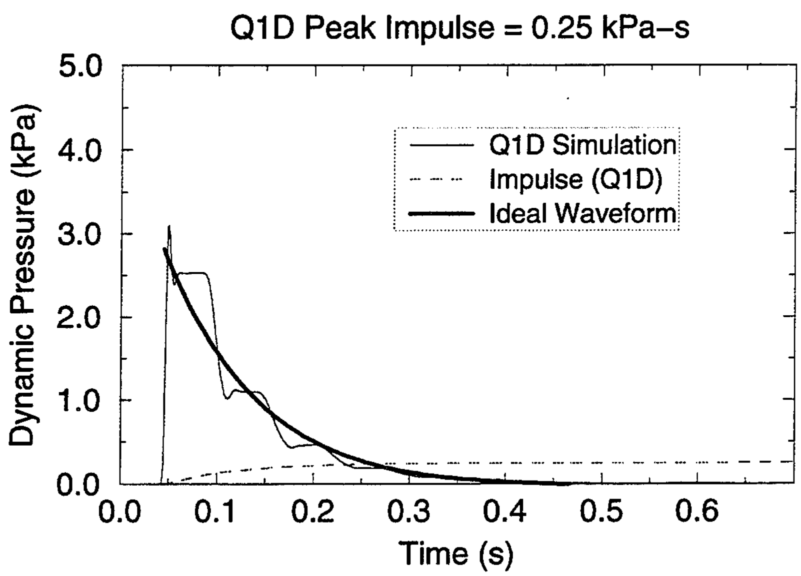

Figure 8. 1.21 MPa (175 psig) Driver Overpressure - Ideal Waveform Based on Dynamic Pressure Impulse.

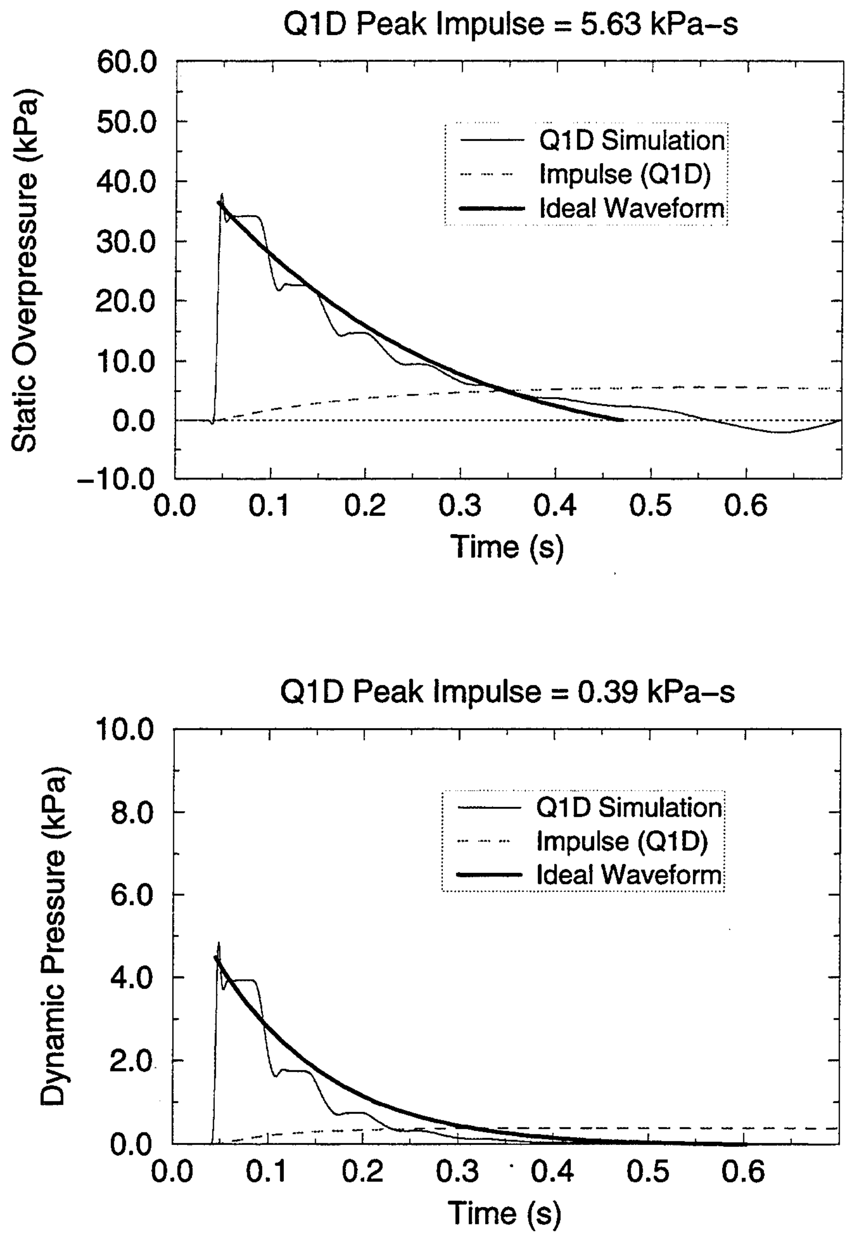

Figure 9. 1.55 MPa (225 psig) Driver Overpressure - Ideal Waveform Based on Static Overpressure Impulse.

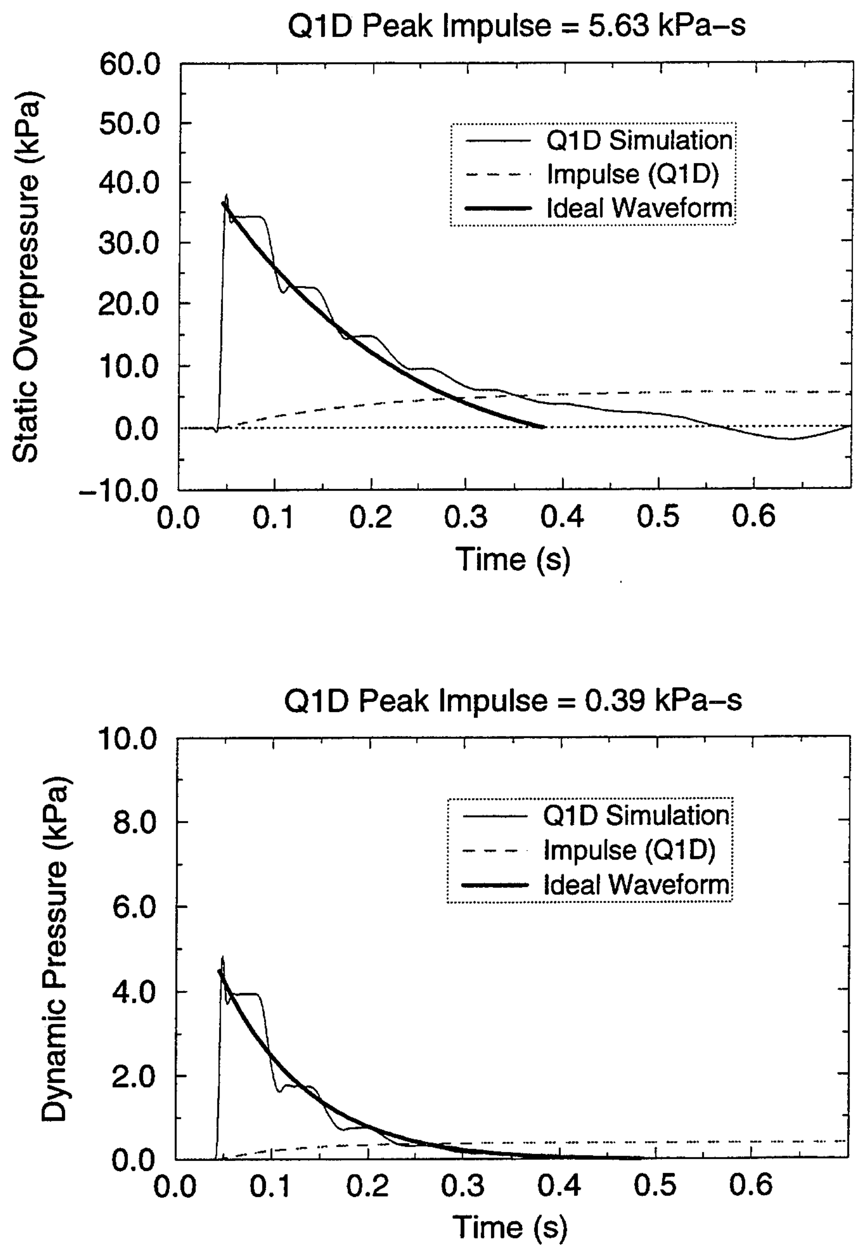

Figure 10. 1.55 MPa (225 psig) Driver Overpressure - Ideal Waveform Based on Dynamic Pressure Impulse.

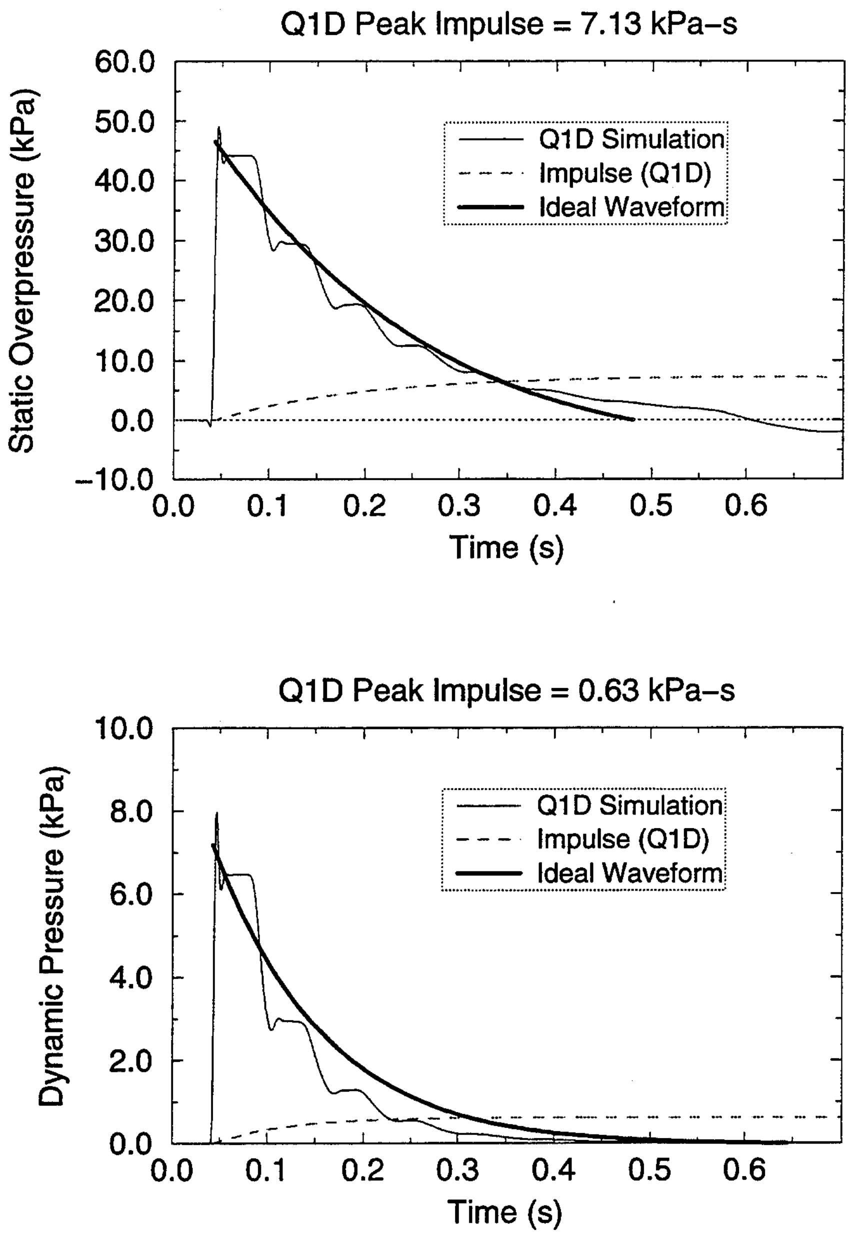

Figure 11. 2.07 MPa (300 psig) Driver Overpressure - Ideal Waveform Based on Static Overpressure Impulse.

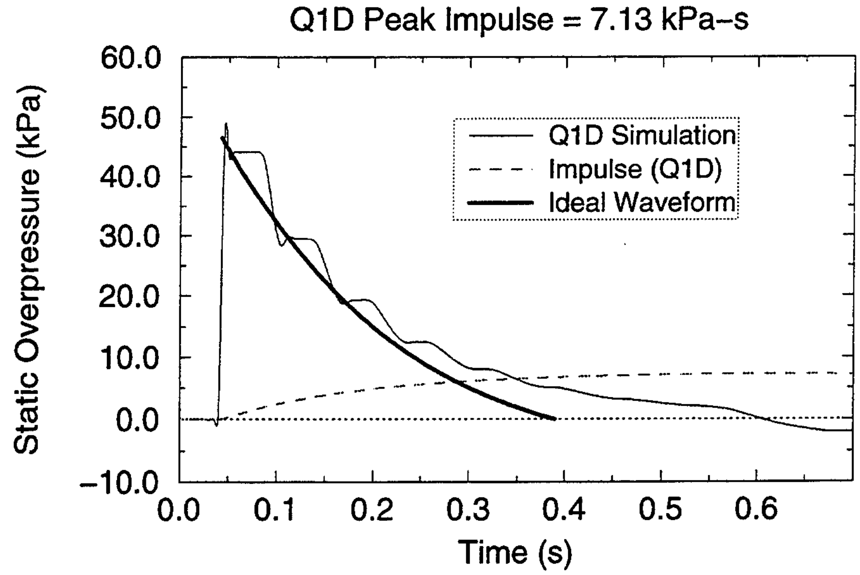

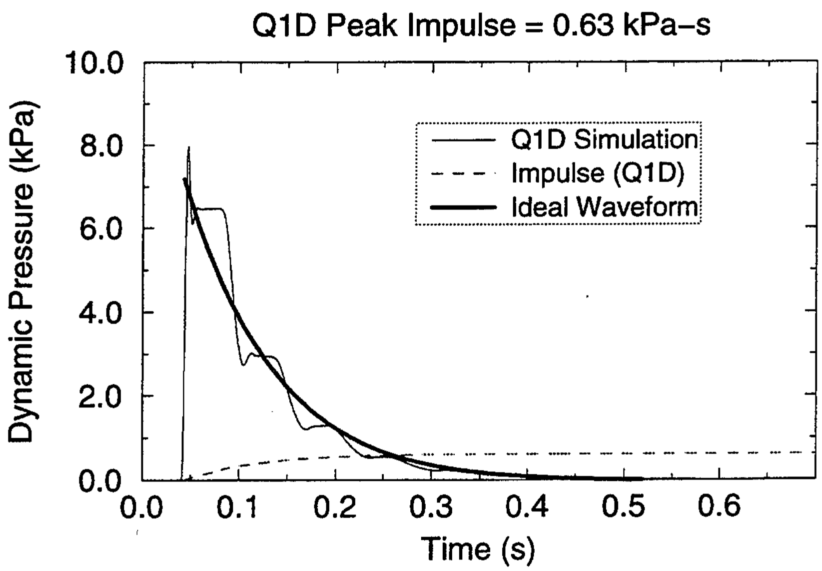

Figure 12. 2.07 MPa (300 psig) Driver Overpressure - Ideal Waveform Based on Dynamic Pressure Impulse.

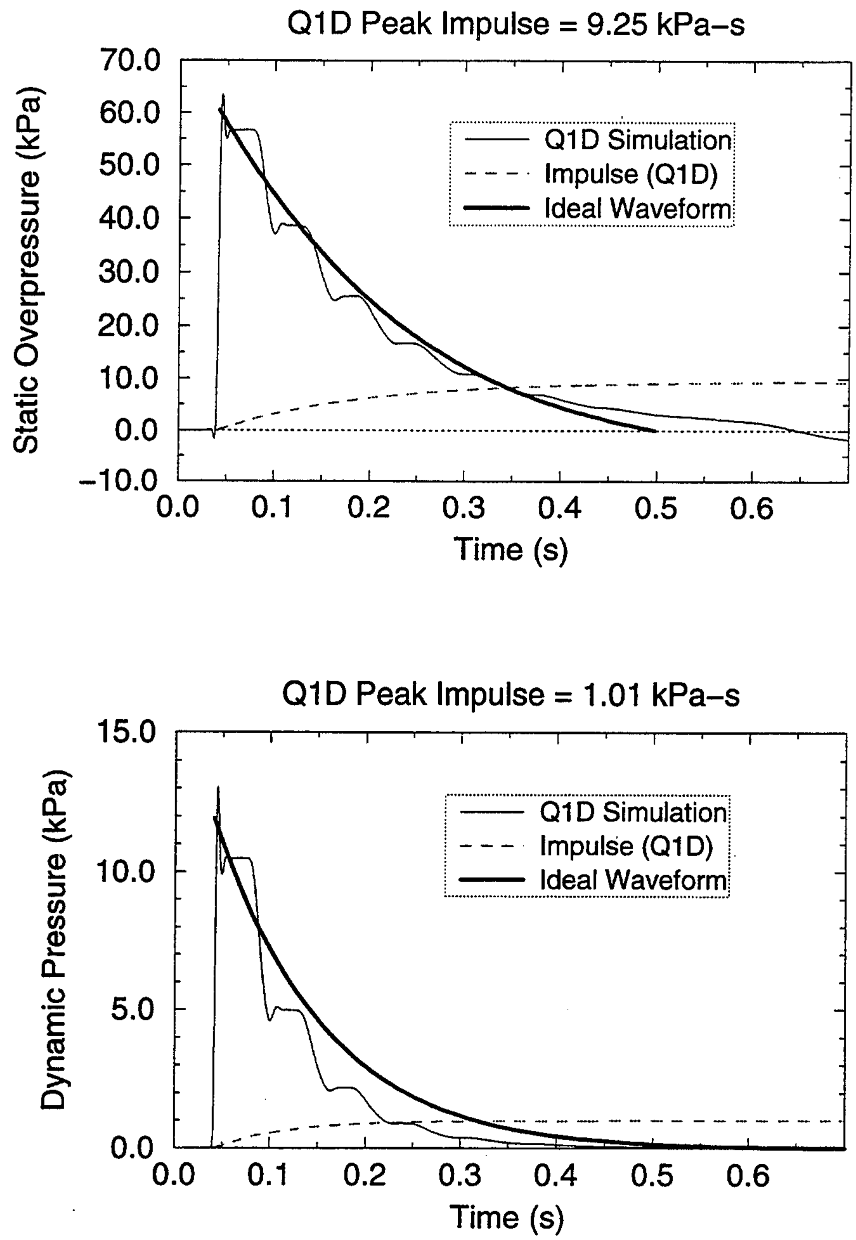

Figure 13. 2.76 MPa (400 psig) Driver Overpressure - Ideal Waveform Based on Static Overpressure Impulse.

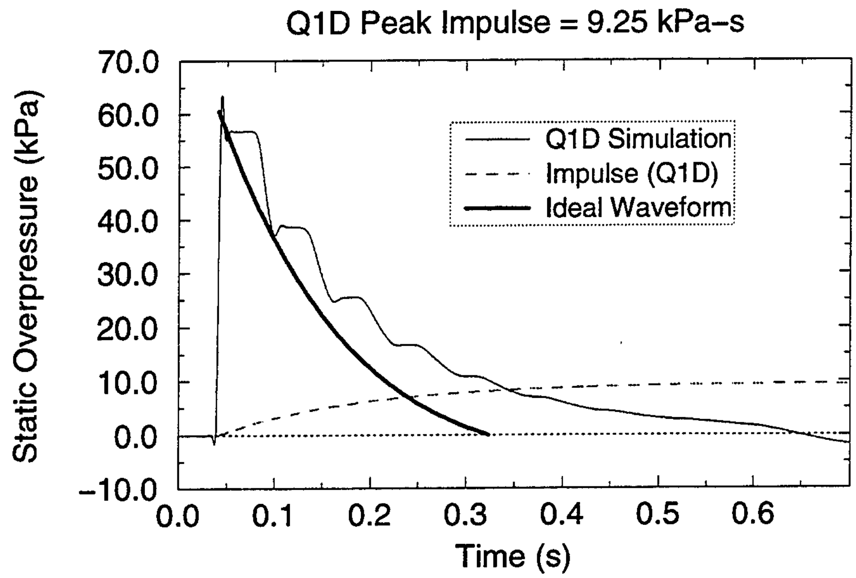

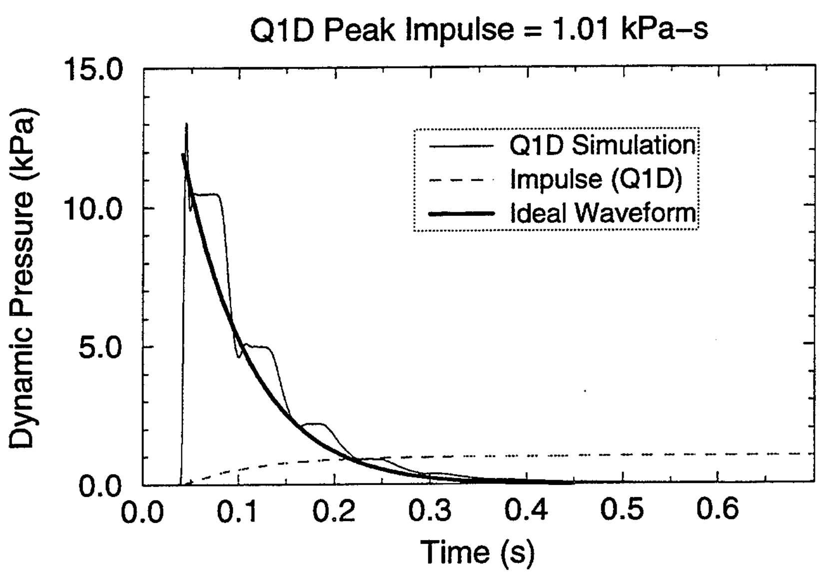

Figure 14. 2.76 MPa (400 psig) Driver Overpressure - Ideal Waveform Based on Dynamic Pressure Impulse.

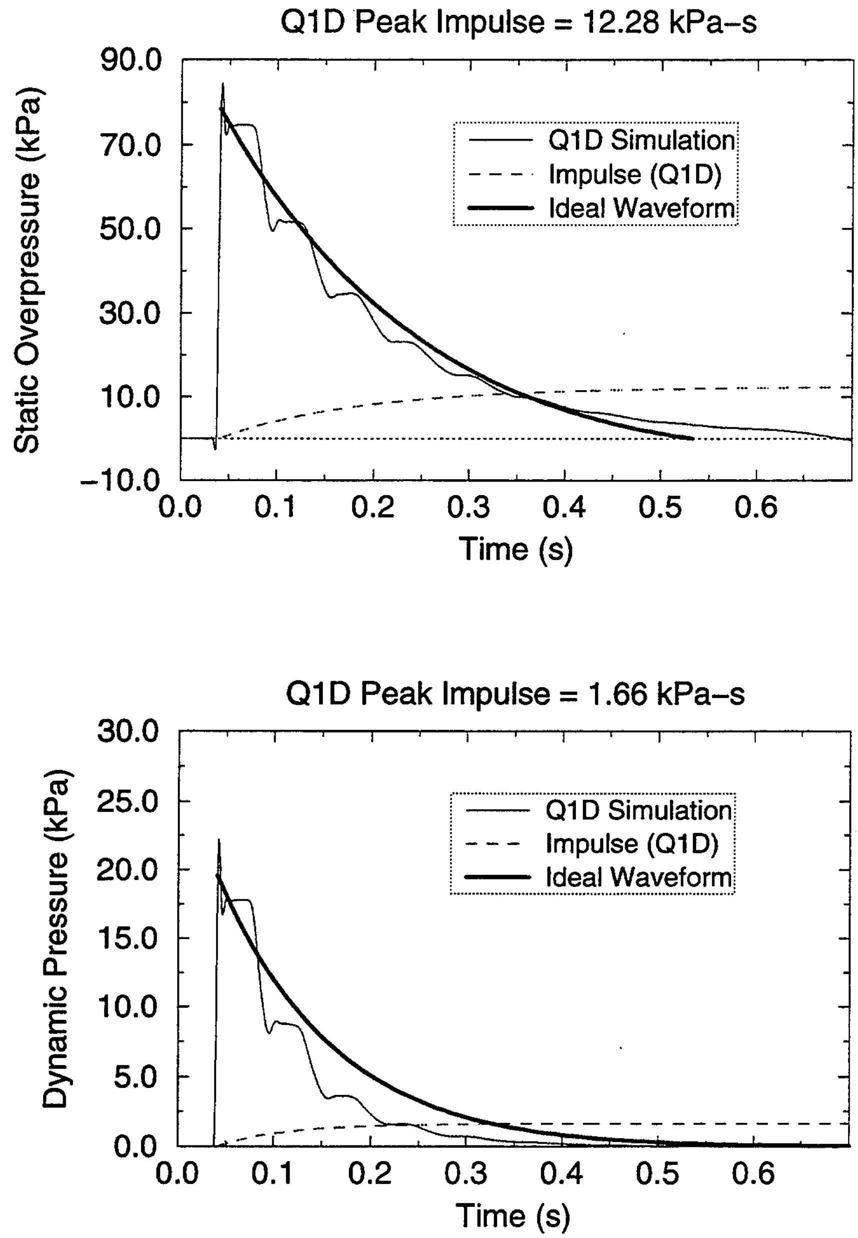

Figure 15. 3.79 MPa (550 psig) Driver Overpressure - Ideal Waveform Based on Static Overpressure Impulse.

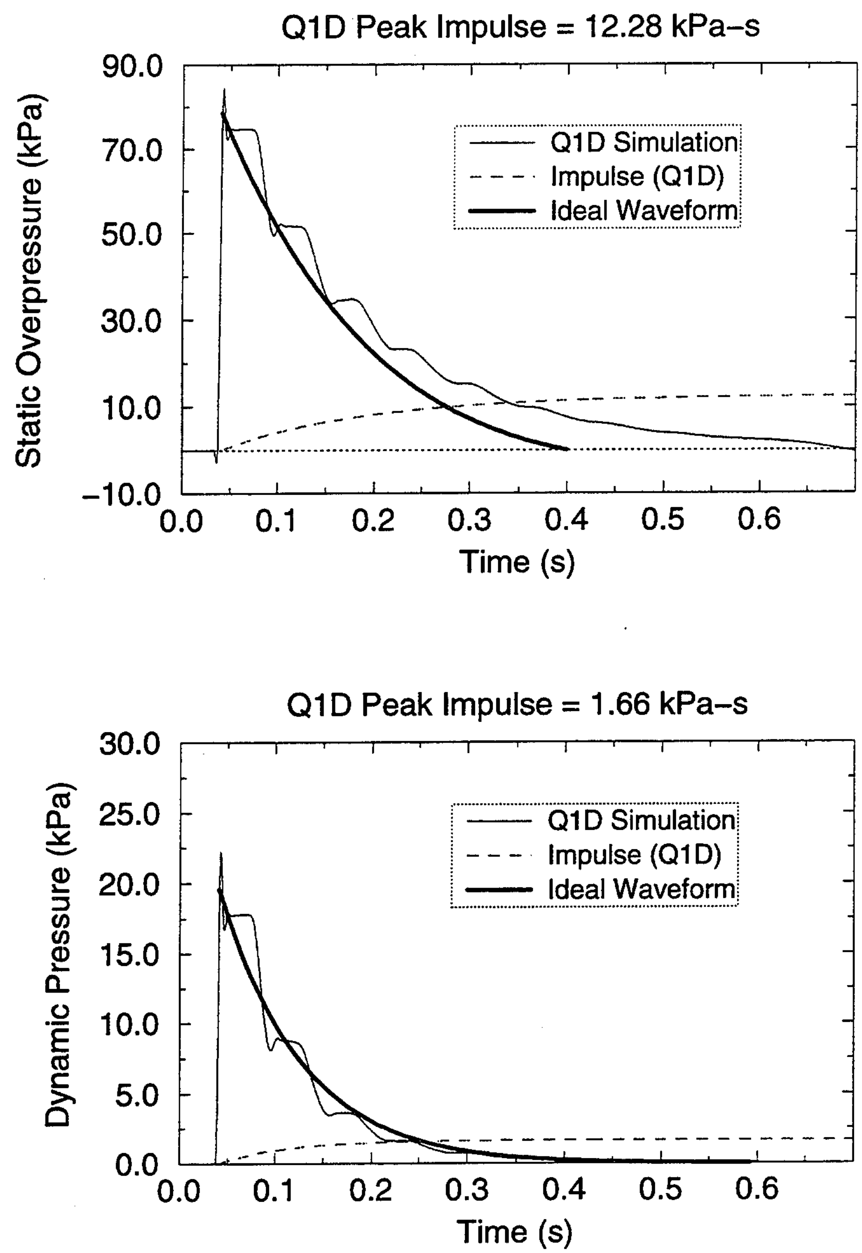

Figure 16. 3.79 MPa (550 psig) Driver Overpressure - Ideal Waveform Based on Dynamic Pressure Impulse.

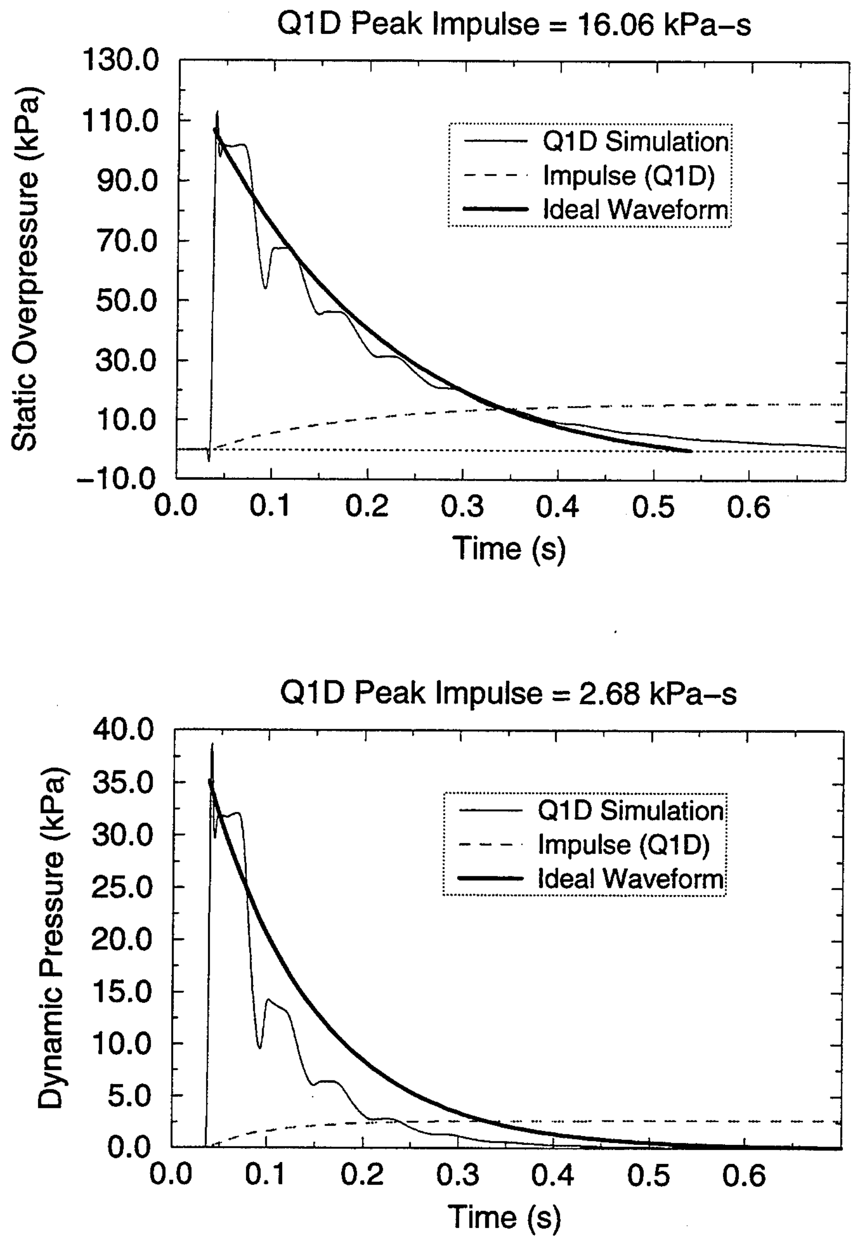

Figure 17. 5.17 MPa (750 psig) Driver Overpressure - Ideal Waveform Based on Static Overpressure Impulse.

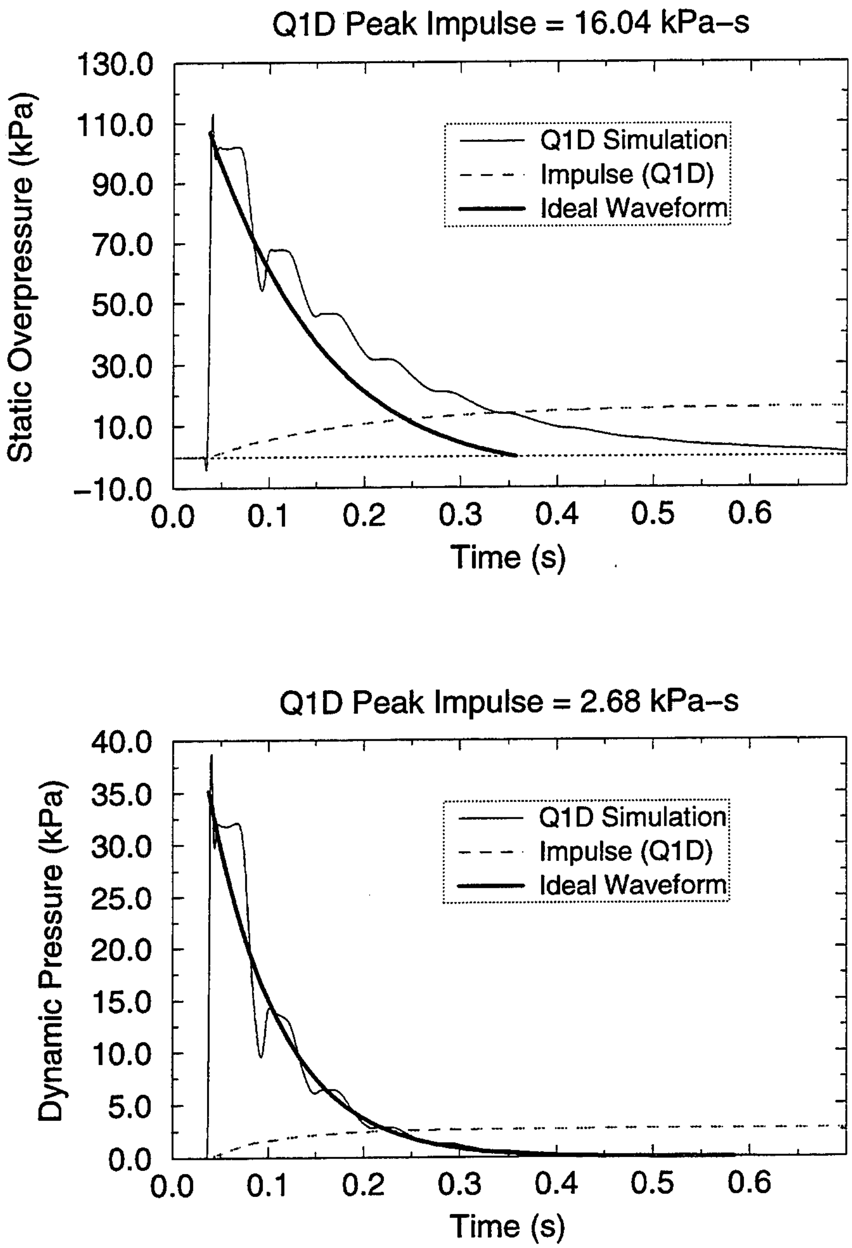

Figure 18. 5.17 MPa (750 psig) Driver Overpressure - Ideal Waveform Based on Dynamic Pressure Impulse.

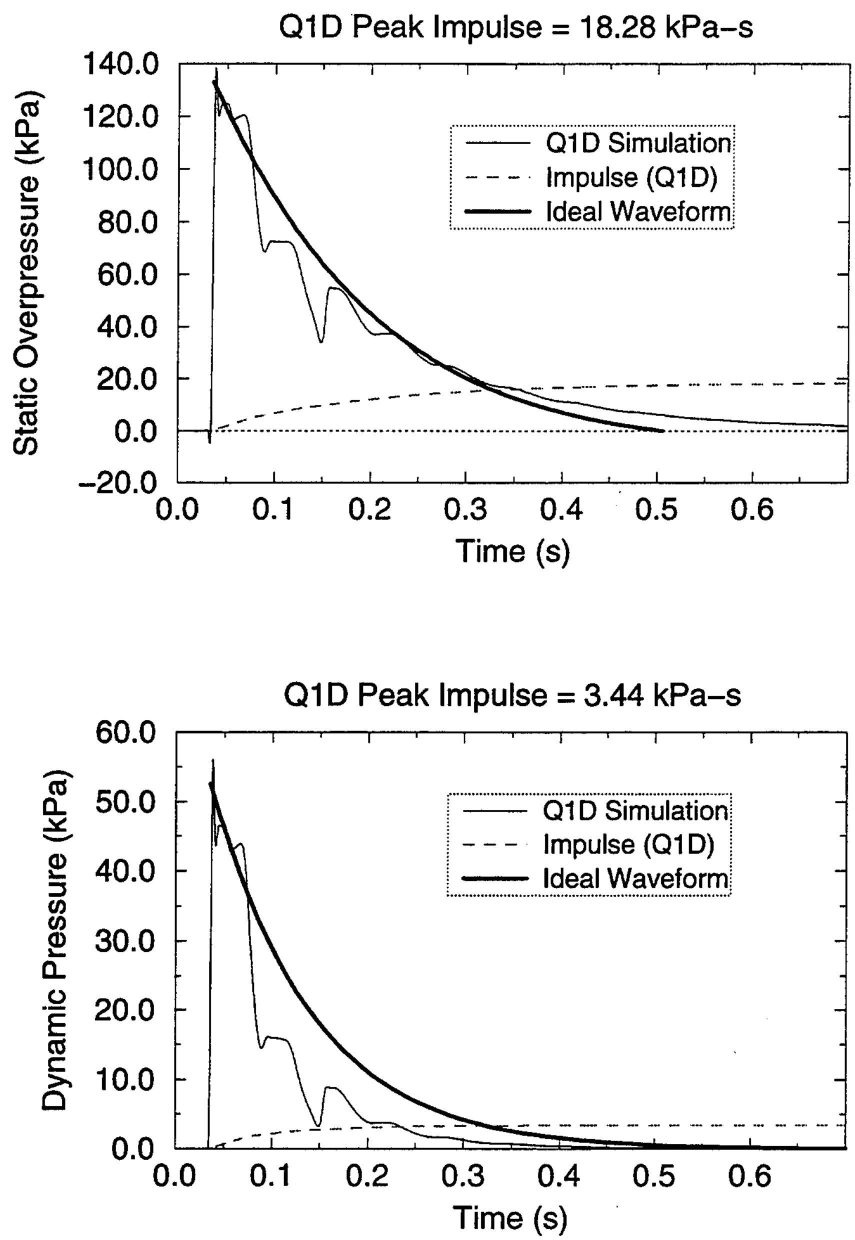

Figure 19. 6.20 MPa (900 psig) Driver Overpressure - Ideal Waveform Based on Static Overpressure Impulse.

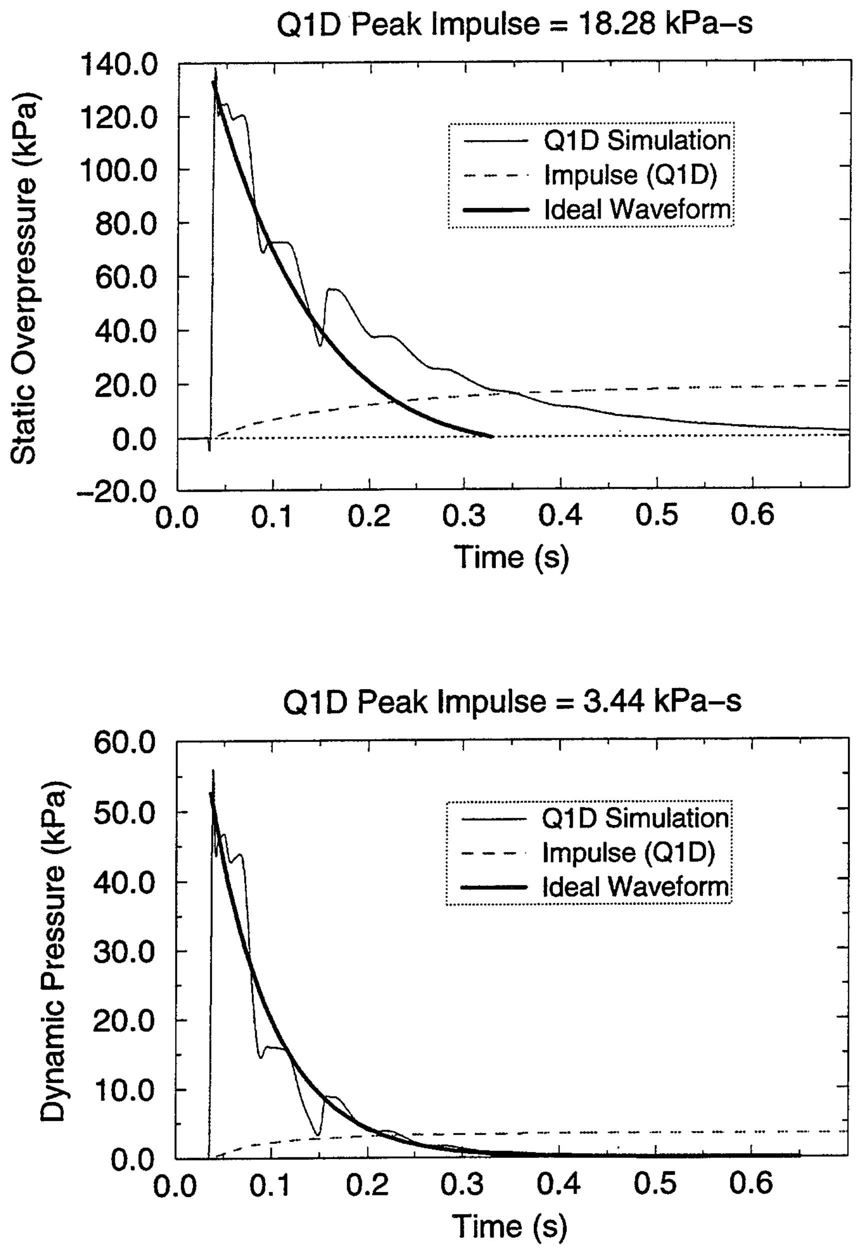

Figure 20. 6.20 MPa (900 psig) Driver Overpressure - Ideal Waveform Based on Dynamic Pressure Impulse.

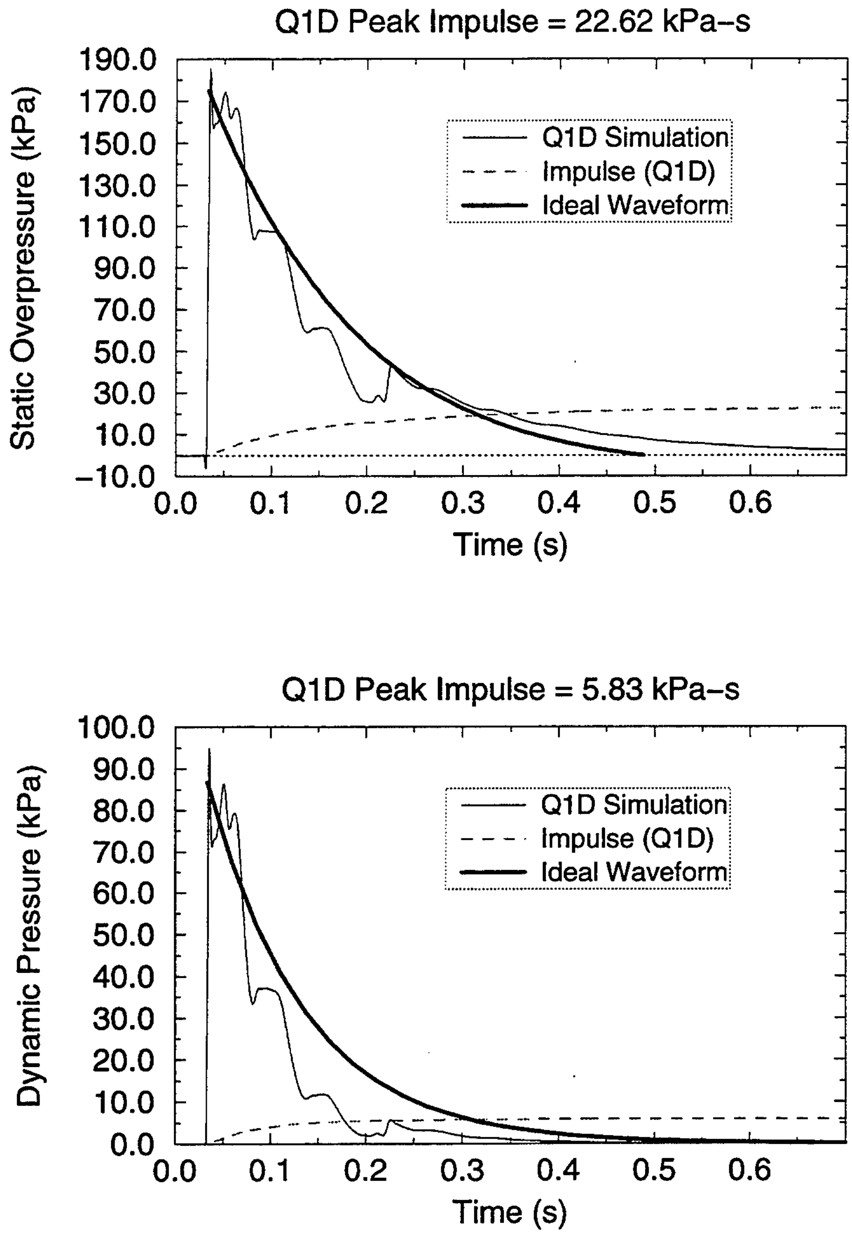

Figure 21. 8.27 MPa (1200 psig) Driver Overpressure - Ideal Waveform Based on Static Overpressure Impulse.

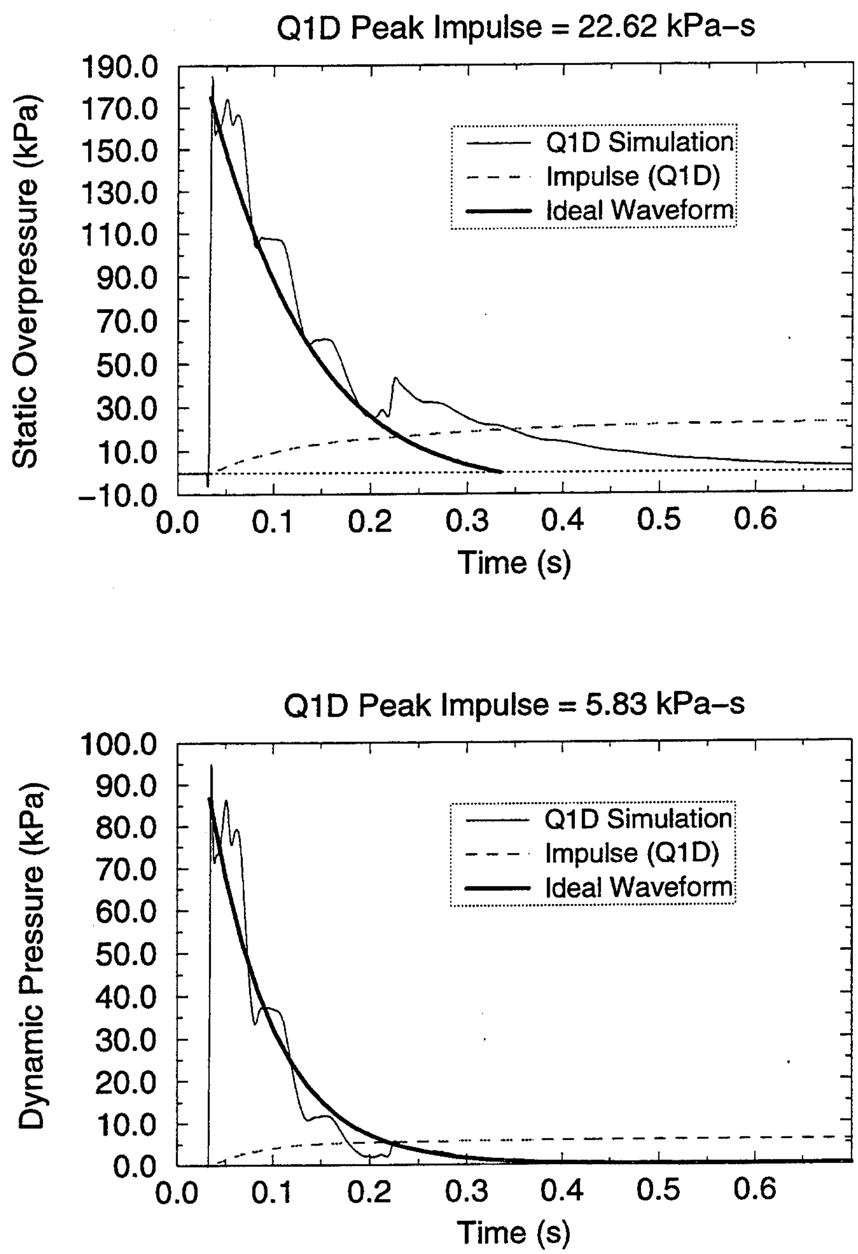

Figure 22. 8.27 MPa (1200 psig) Driver Overpressure - Ideal Waveform Based on Dynamic Pressure Impulse.

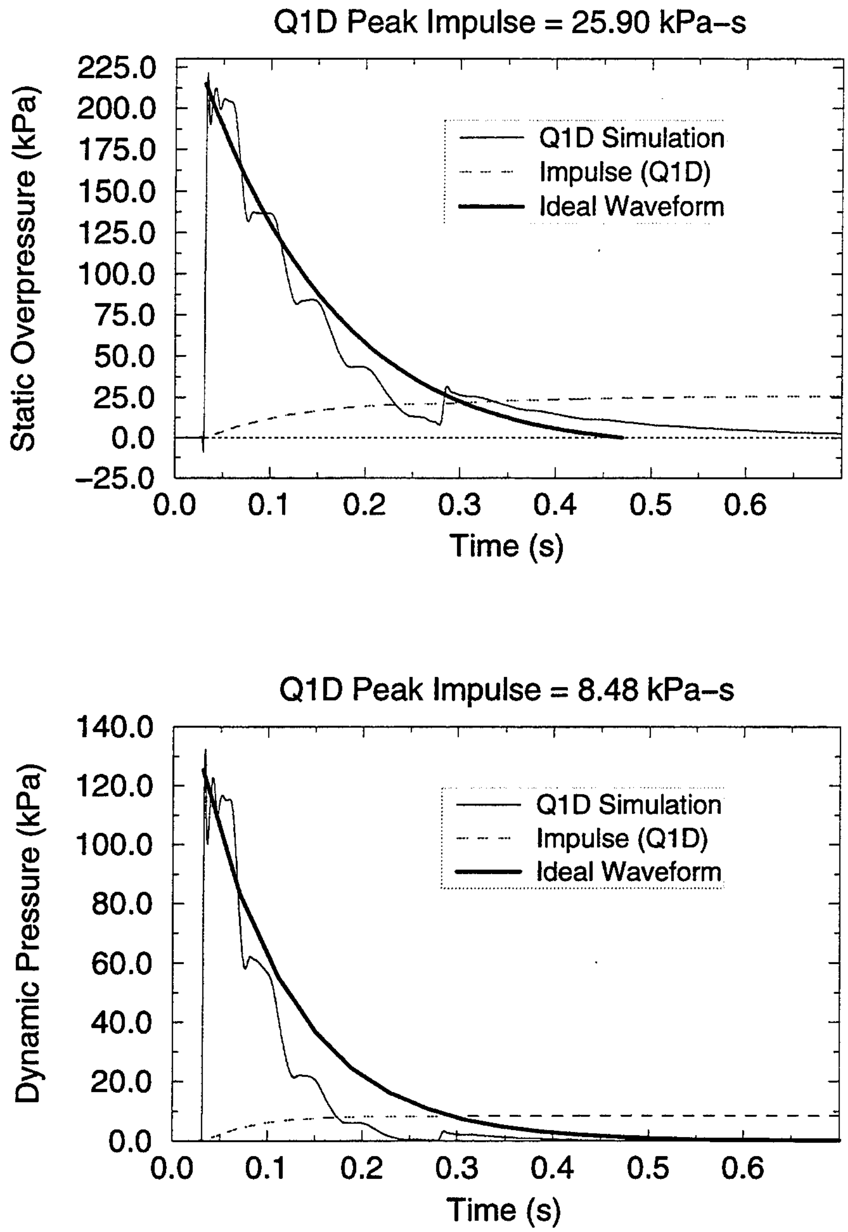

Figure 23. 10.34 MPa (1500 psig) Driver Overpressure - Ideal Waveform Based on Static Overpressure Impulse.

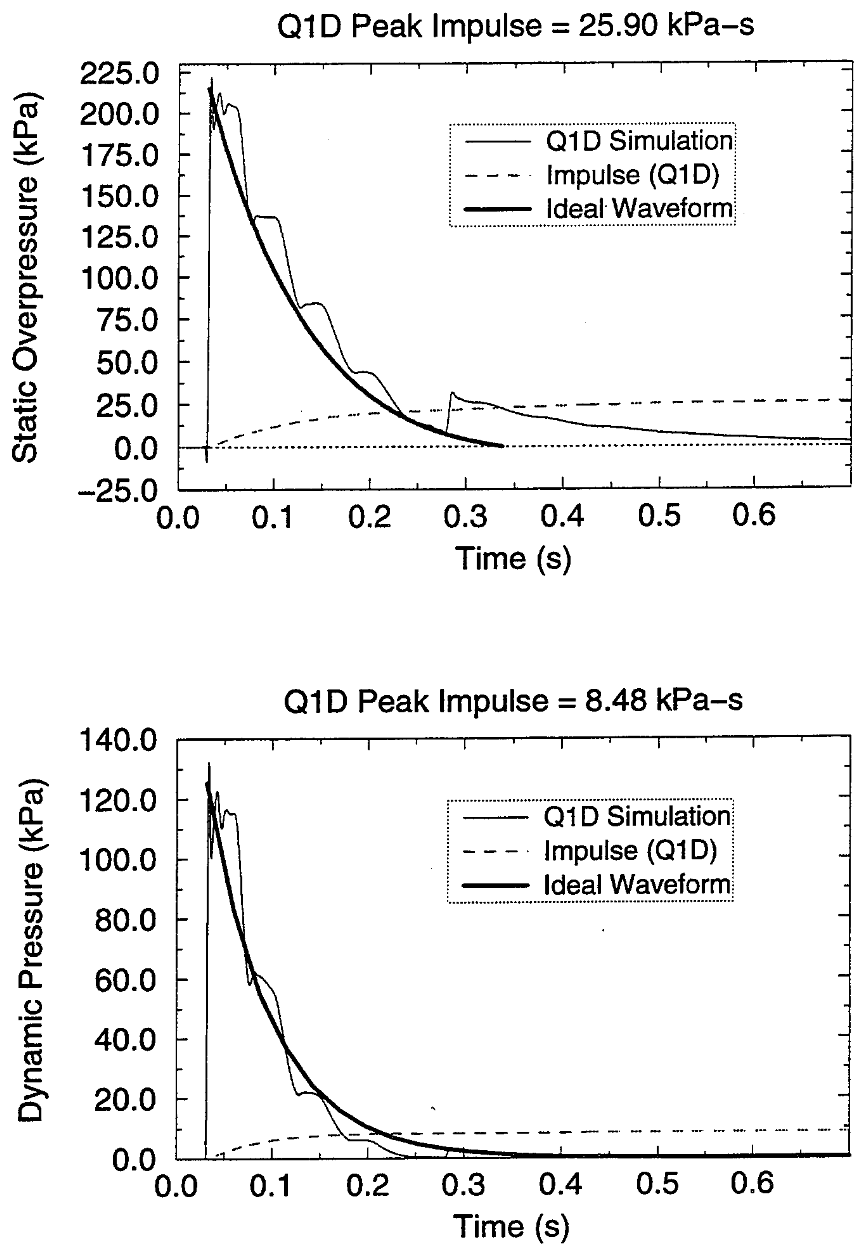

Figure 24. 10.34 MPa (1500 psig) Driver Overpressure - Ideal Waveform Based on Dynamic Pressure Impulse.

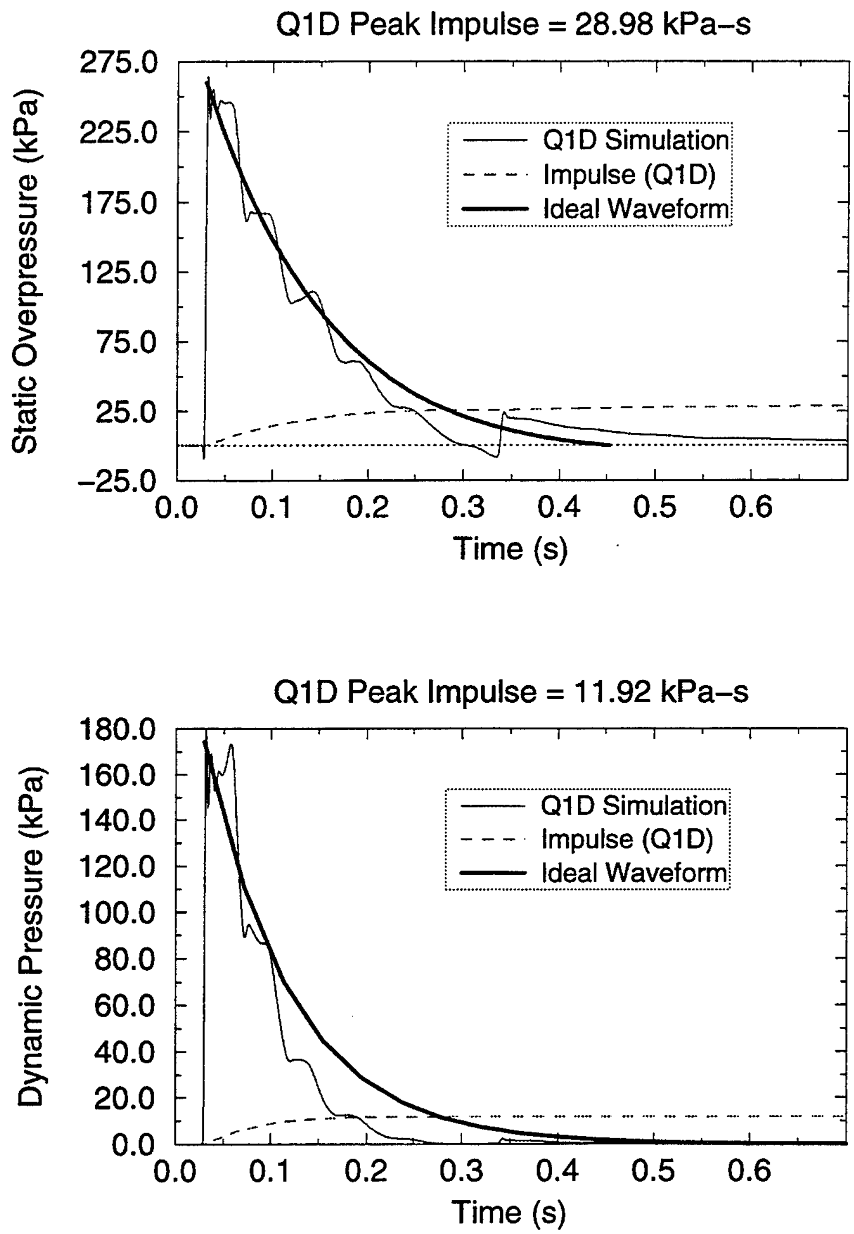

Figure 25. 12.75 MPa (1850 psig) Driver Overpressure - Ideal Waveform Based on Static Overpressure Impulse.

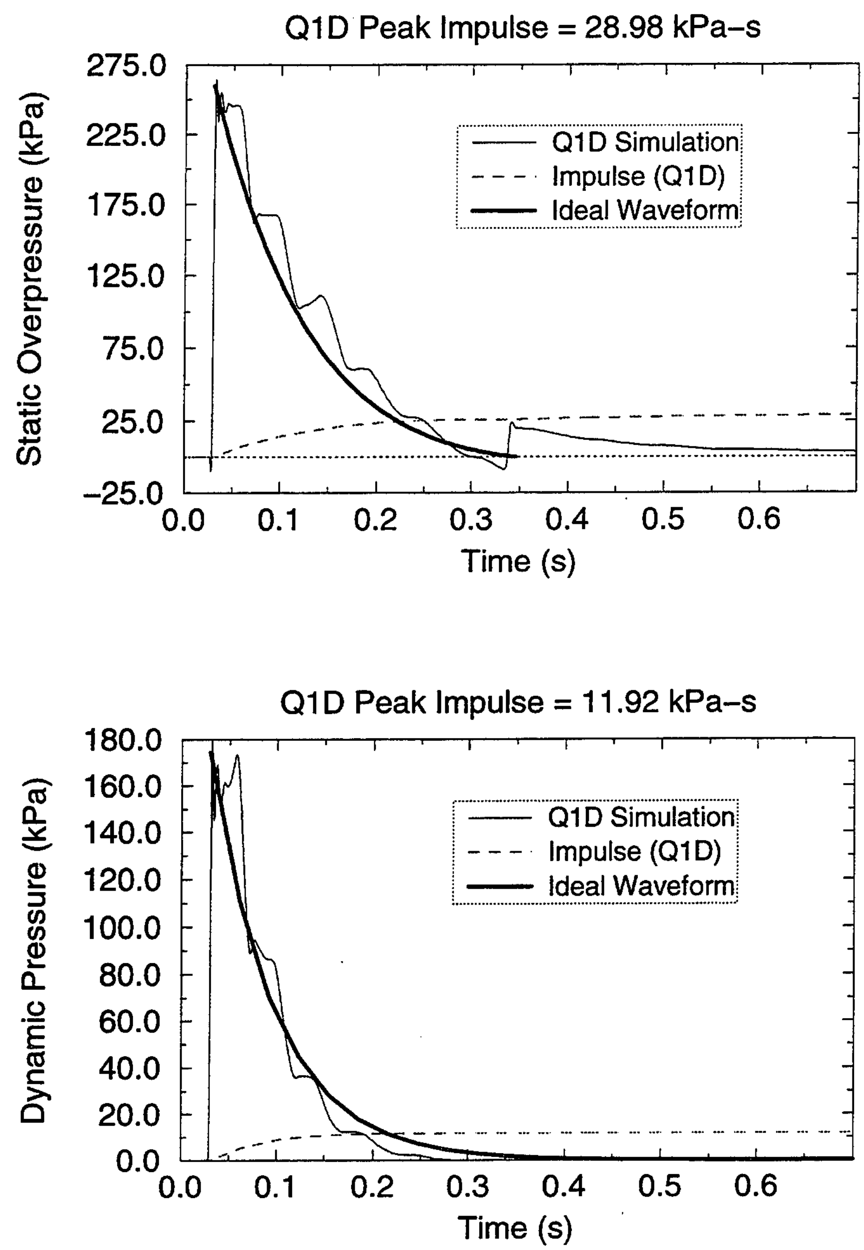

Figure 26. 12.75 MPa (1850 psig) Driver Overpressure - Ideal Waveform Based on Dynamic Pressure Impulse.

REFERENCES

Glass, I.I., and J.Gordon Hall. "Handbook of Supersonic Aerodynamics - Section 18 - Shock Tubes." NAVORD Report 1488 (Vol.6), Department of the Navy, December 1959.

Glasstone, S., and P. Dolan - Editors. "The Effects of Nuclear Weapons." Department of Army Pamphlet No. 50-3, HQ, Department of Army, March 1977.

Opalka, K.O. "Large Blast-Wave Simulators (LBS) with Cold-Gas Drivers: Computational Design Studies." BRL-TR-2786, U.S. Army Ballistic Research Laboratory, Aberdeen Proving Ground, Maryland 21005, March 1987.

Opalka, K.O. "Optical Studies of the Flow Start-up Processes in Four Convergent-Divergent Nozzles." BRL-TR-3215, U.S. Army Ballistic Research Laboratory, Aberdeen Proving Ground, Maryland 21005, March 1991.

Opalka, K.O., and A. Mark. "The BRL-Q1D Code: A Tool for the Numerical Simulation of Flows in Shock Tubes with Variable Cross-Sectional Areas." BRL-TR-2763, U.S. Army Ballistic Research Laboratory, Aberdeen Proving Ground, Maryland 21005, October 1986.

Opalka, K.O., and R.J. Pearson, "Advanced Design Concepts for a Large Blast/Thermal Simulator," Proceedings of the 11th International Symposium on Military Applications of Blast Simulation, Albuquerque, NM, September 1989.

Pearson, R.J., S.J. Schraml, K.O. Opalka. "Development of the BRL Probative Tube." Proceedings of the 12th International Symposium on the Military Applications of Blast Simulation, Centre d'Etudes de Gramat, 46500 Gramat, France, September 1991.

Schraml, S.J., and R.J. Pearson, "Computer Programs for LB/TS Test Design: Technical Description, Usage Instructions and Source Code Listings." ARL-MR-260, U.S. Army Research Laboratory, Aberdeen Proving Ground, Maryland 21005, September 1995.

Smiley, R., J. Ruetenik, and M. Tomayko."Reflect-4 Code Computations of 40 KT Nuclear Blast Waves Reflected from the Ground." DNA-TR-81-203-V1, Defense Nuclear Agency, Washington, DC. November 1982.

INTENTIONALLY LEFT BLANK

NO. OF COPIES	ORGANIZATION
2	ADMINISTRATOR DEFENSE TECHNICAL INFO CENTER ATTN DTIC DDA 8725 JOHN J KINGMAN RD STE 0944 FT BELVOIR VA 22060-6218
1	DIRECTOR US ARMY RESEARCH LABORATORY ATTN AMSRL OP SD TA/ RECORDS MANAGEMENT 2800 POWDER MILL RD ADELPHI MD 20783-1197
1	DIRECTOR US ARMY RESEARCH LABORATORY ATTN AMSRL OP SD TL/ TECHNICAL LIBRARY 2800 POWDER MILL RD ADELPHI MD 207830-1197
1	DIRECTOR US ARMY RESEARCH LABORATORY ATTN AMSRL OP SD TP/ TECH PUBLISHING BRANCH 2800 POWDER MILL RD ADELPHI MD 20783-1197
2	HQDA (SARD TR/MS K KOMINOS) (SARD TR/DR R CHAIT) WASHINGTON DC 20310-0103
2	DIRECTOR FEDERAL EMERGENCY MGMT AGENCY ATTN PUBLIC RELATIONS OFFICE TECHNICAL LIBRARY WASHINGTON DC 20472
2	HQDA (SARD TT/MS C NASH) (SARD TT/DR F MILTON) WASHINGTON DC 20310-0103
1	CHAIRMAN DOD EXPLOSIVES SAFETY BOARD ROOM 856 C HOFFMAN BLDG 1 2461 EISENHOWER AVENUE ALEXANDRIA VA 22331-0600
1	DIRECTOR OF DEFENSE RESEARCH AND ENGINEERING ATTN DD/TWP WASHINGTON DC 20301

NO. OF COPIES	ORGANIZATION
1	DIRECTOR DEFENSE INTELLIGENCE AGENCY ATTN DT 2/WPNS & SYS DIVISION WASHINGTON DC 20301
1	ASST SECRETARY OF DEFENSE (ATOMIC ENERGY ATTN DOCUMENT CONTROL WASHINGTON DC 20301
6	DIRECTOR DEFENSE NUCLEAR AGENCY ATTN CSTI TECHNICAL LIBRARY ESA W SUMMA E SEIDEN K PETERSEN WEP T KENNEDY M FRANKEL WASHINGTON DC 20305
1	CHAIRMAN JOINT CHIEFS OF STAFF ATTN J 5 R&D DIVISION WASHINGTON DC 20301
2	DA DCSOPS ATTN TECHNICAL LIBRARY DIR OF CHEM & NUC OPS WASHINGTON DC 20310
4	COMMANDER FIELD COMMAND DNA ATTN FCTTS E MARTINEZ FCTOSL F MOYNIHAN FCTIH H ROSS FCTIH W BRENNAN KIRTLAND AFB NM 87115
1	EUROPEAN RESEARCH OFFICE USARDSG (UK) ATTN DR R REICHENBACH BOX 65 FPO NEW YORK 09510-1500
10	CENTRAL INTELLIGENCE AGENCY DIR/DB/STANDARD ATTN GE 47 HQ WASHINGTON DC 20505
1	DIRECTOR ADVANCED RSCH PROJECTS AGENCY ATTN TECHNICAL LIBRARY 3701 NORTH FAIRFAX DRIVE ARLINGTON VA 22203-1714

NO. OF COPIES	ORGANIZATION
2	COMMANDER US ARMY NRDEC ATTN AMSNA D DR D SIELING STRNC UE J CALLIGEROS NATICK MA 01762
2	COMMANDER US ARMY CECOM ATTN AMSEL RD AMSEL RO TPPO P FORT MONMOUTH NJ 07703-5301
1	COMMANDER US ARMY CECOM R&D TECHNICAL LIBRARY ATTN ASQNC ELC IS L R MYER CTR FORT MONMOUTH NJ 07703-5000
1	MIT ATTN TECHNICAL LIBRARY CAMBRIDGE MA 02139
1	COMMANDER US ARMY FSTC ATTN RESEARCH & DATA BRANCH 220 7TH STREET NE CHARLOTTESVILLE VA 22901-5396
1	COMMANDER US ARMY ARDEC ATTN SMCAR FSM W/BARBER BLDG94 PICATINNY ARSENAL NJ 07806-5000
1	DIRECTOR US ARMY TRAC FT LEE ATTN ATRC L MR CAMERON FORT LEE VA 23801-6140
1	DIRECTOR US ARMY MISSILE & SPACE INTELLIGENCE CENTER ATTN AIAMS YDL REDSTONE ARSENAL AL 35898-5500
1	COMMANDING OFFICER (CODE L51) NAVAL CIVIL ENGINEERING LAB ATTN J TANCRETO PORT HUENEME CA 93043-5003

NO. OF COPIES	ORGANIZATION
2	COMMANDER US ARMY STRATEGIC DEFENSE CMD ATTN CSSD H MPL TECH LIB CSSD H XM DR DAVIES PO BOX 1500 HUNTSVILLE AL 35807
2	COMMANDER US ARMY CORPS OF ENGINEERS WATERWAYS EXPERIMENT STA ATTN CEWES SS R J WATT CEWES TL TECH LIBRARY PO BOX 631 VICKSBURG MS 39180-0631
1	COMMANDER US ARMY ENGINEER DIVISION ATTN HNDED FD PO BOX 1500 HUNTSVILLE AL 35807
3	COMMANDER US ARMY NUCLEAR & CHEM AGENCY 7150 HELLER LOOP SUITE 101 SPRINGFIELD VA 22150-3198
1	COMMANDER US ARMY CORPS OF ENGINEERS FT WORTH DISTRICT ATTN CESWF PM J PO BOX 17300 FORT WORTH TEXAS 76102-0300
1	DIRECTOR TRAC FLVN ATTN ATRC FORT LEAVENWORTH KS 66027-5200
1	COMMANDER US ARMY RESEARCH OFFICE ATTN SLCRO D PO BOX 12211 RESEARCH TRIANGLE PARK NC 27709-2211
1	DIRECTOR HQ TRAC RPD ATTN ATRC RPR RADDA FORT MONROE VA 23651-5143
2	OFFICE OF NAVAL RESEARCH ATTN DR A FAULSTICK CODE 23 800 N QUINCY STREET ARLINGTON VA 22217

NO. OF COPIES	ORGANIZATION
1	DIRECTOR TRAC WSMR ATTN ATRC WC KIRBY WSMR NM 88002-5502
2	COMMANDER US ARMY WSMR ATTN STEWS NED (DR MEASON) STEWS DATTS O (RL PENNY) WSMR NM 88002-5158
2	CHIEF OF NAVAL OPERATIONS DEPARTMENT OF THE NAVY ATTN OP 03EG OP 985F WASHINGTON DC 20350
1	COMMANDER DAVID TAYLOR RESEARCH CENTER ATTN CODE 522 TECH INFO CTR BETHESDA MD 20084-5000
1	OFFICER IN CHARGE (CODE L31) CIVIL ENGINEERING LABORATORY NAVAL CONST BATTALION CENTER ATTN TECHNICAL LIBRARY PORT HUENEME CA 93041
1	COMMANDING OFFICER WHITE OAK WARFARE CENTER ATTN CODE WA501 NNPO SILVER SPRING MD 20902-5000
1	COMMANDER (CODE 533) NAVAL WEAPONS CENTER ATTN TECHNICAL LIBRARY CHINA LAKE CA 93555-6001
1	COMMANDER DAHLGREN DIVISION NAVAL SURFACE WARFARE CENTER ATTN CODE E23 LIBRARY DAHLGREN VA 22448-5000
1	COMMANDER NAVAL RESEARCH LABORATORY ATTN CODE 2027 TECH LIBRARY WASHINGTON DC 20375
1	OFFICER IN CHARGE WHITE OAK WARFARE CENTER DETACHMENT ATTN CODE E232 TECH LIBRARY 10901 NEW HAMPSHIRE AVENUE SILVER SPRING MD 20903-5000

NO. OF COPIES	ORGANIZATION
1	AL/LSCF ATTN J LEVINE EDWARDS AFB CA 93523-5000
1	COMMANDER NAVAL WEAPONS EVALUATION FAC ATTN DOCUMENT CONTROL KIRTLAND AFB NM 87117
1	RADC (EMTLD/DOCUMENT LIB) GRIFFISS AFB NY 13441
1	AEDC ATTN R MCAMIS MAIL STOP 980 ARNOLD AFB TN 37389
1	OLAC PL/TSTL ATTN D SHIPLETT EDWARDS AFB CA 93523 5000
1	AFIT/ENY ATTN LTC HASEN PHD WRIGHT PATTERSON AFB OH 45433-6583
2	AIR FORCE ARMAMENT LAB ATTN AFATL/DOIL AFATL/DLYV EGLIN AFB FL 32542-5000
1	DIRECTOR IDAHO NATIONAL ENGINEERING LAB ATTN SPEC PROGRAMS J PATTON 2151 NORTH BLVD MS 2802 IDAHO FALLS ID 83415
3	PHILLIPS LABORATORY (AFWL) ATTN NTE NTED NTES KIRTLAND AFB NM 87117-6008
1	DIRECTOR LAWRENCE LIVERMORE NATL LAB ATTN TECH INFO DEPT L 3 PO BOX 808 LIVERMORE CA 94550
1	AFIT ATTN TECHNICAL LIBRARY BLDG 640/B WRIGHT PATTERSON AFB OH 45433

NO. OF COPIES	ORGANIZATION
1	DIRECTOR NATL AERONAUTICS & SPACE ADMIN ATTN SCIENTIFIC & TECH INFO FAC PO BOX 8757 BWI AIRPORT BALTIMORE MD 21240
1	FTD/NIIS WRIGHT PATTERSON AFB OH 45433
3	KAMAN SCIENCES CORPORATION ATTN LIBRARY PA ELLIS FH SHELTON PO BOX 7463 COLORADO SPRINGS CO 80933-7463
4	DIRECTOR IDAHO NATIONAL ENGINEERING LAB EG&G IDAHO INC ATTN R GUENZLER MS 3505 R HOLMAN MS 3510 R A BERRY W C REED PO BOX 1625 IDAHO FALLS ID 83415
4	DIRECTOR SANDIA NATIONAL LABORATORIES ATTN DOC CONTROL 3141 D GARDNER DIV 1421 J MCGLAUN DIV 1541 PO BOX 5800 ALBUQUERQUE NM 87185-5800
2	LOS ALAMOS NATL LABORATORY MAIL STATION 5000 REPORT COLLECTION CID 14 MS P364 PO BOX 1663 LOS ALAMOS NM 87545
1	REPORT COLLECTION CIC 14 MS P364 LOS ALAMOS NATL LABORATORY LOS ALAMOS NM 87545
1	REPORT COLLECTION RESEARCH LIBRARY MS P362 PO BOX 7113 LOS ALAMOS NM 87544-7113

NO. OF COPIES	ORGANIZATION
1	DIRECTOR SANDIA NATIONAL LABORATORIES LIVERMORE LABORATORY ATTN DOC CONTROL FOR TECH LIB PO BOX 969 LIVERMORE CA 94550
1	DIRECTOR NASA AMES RESEARCH CENTER APPLIED COMPUTATIONAL AERO BR ATTN DR T HOLTZ MS 202 14 MOFFETT FIELD CA 94035
1	DIRECTOR NASA LANGLEY RESEARCH CENTER ATTN TECHNICAL LIBRARY HAMPTON VA 23665
2	APPLIED RESEARCH ASSOCIATES INC ATTN J KEEFER NH ETHRIDGE PO BOX 548 ABERDEEN MD 21001
4	APPLIED RESEARCH ASSOCIATES INC ATTN C NEEDHAM J CREPEAU S HIKIDA R NEWELL 4300 SAN MATEO BLVD ALBUQUERQUE NM 87110
1	ADA TECHNOLOGIES INC ATTN JAMES R BUTZ HONEYWELL CENTER SUITE 110 304 INVERNESS WAY SOUTH ENGLEWOOD CO 80112
1	CARPENTER RESEARCH CORP ATTN H JERRY CARPENTER 27520 HAWTHORNE BLVD SUITE 263 PO BOX 2490 ROLLING HILLS ESTATES CA 90274
1	AEROSPACE CORPORATION ATTN TECH INFO SERVICES PO BOX 92957 LOS ANGELES CA 90009
1	THE BOEING COMPANY ATTN AEROSPACE LIBRARY PO BOX 3707 SEATTLE WA 98124

NO. OF COPIES	ORGANIZATION
2	FMC CORPORATION ADVANCED SYSTEMS CENTER ATTN J DROTLEFF C KREBS MDP 95 BOX 58123 2890 DE LA CRUZ BLVD SANTA CLARA CA 95052
1	SVERDRUP TECHNOLOGY INC SVERDRUP CORPORATION AEDC ATTN BD HEIKKINEN MS 900 ARNOLD AFB TN 37389-9998
1	DYNAMICS TECHNOLOGY INC ATTN D T HOVE G P MASON 21311 HAWTHORNE BLVD SUITE 300 TORRANCE CA 90503
1	KTECH CORPORATION ATTN DR E GAFFNEY 901 PENNSYLVANIA AVE NE ALBUQUERQUE NM 87111
1	EATON CORPORATION DEFENSE VALVE & ACTUATOR DIV ATTN J WADA 2338 ALASKA AVE EL SEGUNDO CA 90245-4896
2	MCDONNELL DOUGLAS ASTRO- NAUTICS CORP ATTN R W HALPRIN K A HEINLY 5301 BOLSA AVENUE HUNTINGTON BEACH CA 92647
4	KAMAN AVIDYNE ATTN R RUETENIK S CRISCIONE R MILLIGAN T STAGLIANO 83 SECOND AVENUE NORTHWEST INDUSTRIAL PARK BURLINGTON MA 01830
1	MDA ENGINEERING INC ATTN DR DALE ANDERSON 500 EAST BORDER STREET SUITE 401 ARLINGTON TX 07601

NO. OF COPIES	ORGANIZATION
2	POINTWISE INC ATTN J CHAWNER J STEINBRENNER PO BOX 210698 BEDFORD TX 76095-7698
2	PHYSICS INTERNATIONAL CORP PO BOX 5010 SAN LEANDRO CA 94577-0599
2	KAMAN SCIENCES CORPORATION ATTN DASIAC (2CYS) PO DRAWER 1479 816 STATE STREET SANTA BARBARA CA 93102-1479
1	LOGICON RDA ATTN GP GANONG PO BOX 9377 ALBUQUERQUE NM 87119
1	LOGICON RDA ATTN B LEE 6053 W CENTURY BLVD LOS ANGELES CA 90045
1	LOCKHEED MISSILES & SPACE CO ATTN J J MURPHY DEPT 81 11 BLDG 154 PO BOX 504 SUNNYVALE CA 94086
1	SCIENCE CENTER ROCKWELL INTERNATIONAL CORP ATTN S RAMAKRISHNAN D OTA 1049 CAMINO DOS RIOS PO BOX 2085 THOUSAND OAKS CA 91358
1	METACOMP TECHNOLOGIES INC ATTN S CHAKRAVARTHY 650 WESTLAKE BLVD SUITE 203 WESTLAKE VILLAGE CA 91362
1	ORLANDO TECHNOLOGY INC ATTN D MATUSKA 60 SECOND STREET BLDG 5 SHALIMAR FL 32579

NO. OF COPIES	ORGANIZATION
4	S CUBED A DIVISION OF MAXWELL LABS INC ATTN TECHNICAL LIBRARY R DUFF K PYATT J BARTHEL PO BOX 1620 LA JOLLA CA 92037-1620
1	SAICORPORATION ATTN J GUEST 2301 YALE BLVD SE SUITE E ALBUQUERQUE NM 87106
1	SUNBURST RECOVERY INC ATTN DR C YOUNG PO BOX 2129 STEAMBOAT SPRINGS CO 80477
1	SVERDRUP TECHNOLOGY INC ATTN RF STARR PO BOX 884 TULLAHOMA TN 37388
1	S CUBED A DIVISION OF MAXWELL LABS INC ATTN JAMES SEVIER 2501 YALE BLVD SE ALBUQUERQUE NM 87106
3	SRI INTERNATIONAL ATTN DR GR ABRAHAMSON DR J GRAN DR B HOLMES 333 RAVENWOOD AVENUE MENLO PARK CA 94025
1	TRW BALLISTIC MISSILE DIVISION ATTN H KORMAN MAIL STATION 526/614 PO BOX 1310 SAN BERNADINO CA 92402
1	BATTELLE ATTN TACTEC LIB JN KHIGGINS 505 KING AVENUE COLUMBUS OH 43201-2693
1	THERMAL SCIENCE INC ATTN R FELDMAN 2200 CASSENS DRIVE ST LOUIS MO 63026

NO. OF COPIES	ORGANIZATION
2	DENVER RESEARCH INSTITUTE ATTN J WISOTSKI TECHNICAL LIBRARY PO BOX 10758 DENVER CO 80210
1	STATE UNIVERSITY OF NEW YORK MECH & AEROSPACE ENGINEERING ATTN DR PEYMAN GIVI BUFFALO NY 14260
2	UNIVERSITY OF MARYLAND INST FOR ADV COMPUTER STUDIES ATTN L DAVIS G SOBIESKI COLLEGE PARK MD 20742
1	CALIFORNIA INST OF TECHNOLOGY ATTN T J AHRENS 1201 E CALIFORNIA BLVD PASADENA CA 91109
1	STANFORD UNIVERSITY ATTN DR D BERSHADER DURAND LABORATORY STANFORD CA 94305
1	UNIVERSITY OF MINNESOTA ARMY HIGH PERF COMP RES CTR ATTN DR TAYFUN E TEZDUYAR 1100 WASHINGTON AVE SOUTH MINNEAPOLIS MN 55415
3	SOUTHWEST RESEARCH INSTITUTE ATTN DR C ANDERSON S MULLIN A B WENZEL PO DRAWER 28255 SAN ANTONIO TX 78228-0255
2	COMMANDER US ARMY NRDEC ATTN SSCNC YSD (J ROACH) SSCNC WST (A MURPHY) KANSAS STREET NATICK MA 10760-5018
	ABERDEEN PROVING GROUND
5	DIR ARL ATTN AMSRL OP AP L (TECH LIB) BLDG 305 APG

NO. OF COPIES	ORGANIZATION
1	COMMANDER US ARMY TECOM ATTN AMSTE TE F (L TELETSKI) RYAN BLDG APG
1	COMMANDER US ARMY THAMA ATTN AMSTH TE APG -EA
1	COMMANDER US ARMY TEST CENTER ATTN STEC LI APG
27	DIRECTOR US ARMY RESEARCH LABORATORY ATTN AMSRL SC C C NIETUBICZ AMSRL SC CC C ELLIS D HISLEY P COLLINS T KENDALL R SHEROKE AMSRL SC I W STUREK AMSRL SC S R PEARSON AMSRL SL CM E FIORVANTE AMSRL WT TB R FREY J STARKENBERG K BENJAMIN W LAWRENCE T DORSEY R LOTTERO V SMITH J CONDON L FERGUSON R LOUCKS C MERMAGEN A MIHALCIN P MULLER S SCHRAML J SULLIVAN AMSRL WT PB P PLOSTINS P WEIHNACHT B GUIDOS AMSRL WT TC K KIMSEY